

High Precision Measurements of $\sin^2 \theta_{12}$ in Solar and Reactor Neutrino Experiments

A bhijit Bandyopadhyay¹, Sandhya Choubey^{2;3}, Srubabati Goswami⁴, S.T. Petcov^{3;2;5}

¹Theory Group, Saha Institute of Nuclear Physics, 1/AF, Bidhannagar, Calcutta 700 064, India
²INFN, Sezione di Trieste, Trieste, Italy.

³Scuola Internazionale Superiore di Studi Avanzati, I-34014 Trieste, Italy.

⁴Harish-Chandra Research Institute, Chhatnag Road, Jhusi, Allahabad 211 019, India.

⁵Institute of Nuclear Research and Nuclear Energy, Bulgarian Academy of Sciences, 1784 Sofia, Bulgaria.

Abstract

We discuss the possibilities of high precision measurement of the solar neutrino mixing angle $\sin^2 \theta_{12}$ in solar and reactor neutrino experiments. The improvements in the determination of $\sin^2 \theta_{12}$, which can be achieved with the expected increase of statistics and reduction of systematic errors in the currently operating solar and KamLAND experiments, are summarized. The potential of LowNu e elastic scattering experiment, designed to measure the pp solar neutrino flux, for high precision determination of $\sin^2 \theta_{12}$, is investigated in detail. The accuracy in the measurement of $\sin^2 \theta_{12}$, which can be achieved in a reactor experiment with a baseline $L = (50 - 70)$ km, corresponding to a Survival Probability Minimum (SPM) $\sin^2 \theta_{13}$, is thoroughly studied. We include the effect of the uncertainty in the value of $\sin^2 \theta_{13}$ in the analyses. A LowNu measurement of the pp neutrino flux with a 1% error would allow to determine $\sin^2 \theta_{12}$ with an error of 14% (17%) at 3 σ from a two-generation (three-generation) analysis. The same parameter $\sin^2 \theta_{12}$ can be measured with an uncertainty of 2% (6%) at 1 σ (3 σ) in a reactor experiment with $L = 60$ km, statistics of 60 GW kT y and systematic error of 2%. For the same statistics, the increase of the systematic error from 2% to 5% leads to an increase in the uncertainty in $\sin^2 \theta_{12}$ from 6% to 9% at 3 σ . The inclusion of the $\sin^2 \theta_{13}$ uncertainty in the analysis changes the error on $\sin^2 \theta_{12}$ to 3% (9%). The effect of $\sin^2 \theta_{13}$ uncertainty on the $\sin^2 \theta_{12}$ measurement in both types of experiments is considerably smaller than naively expected.

1 Introduction

There has been a remarkable progress in the studies of neutrino oscillations in the last several years. The experiments with solar, atmospheric and reactor neutrinos [1, 2, 3, 4, 5, 6, 7] have provided compelling evidences for the existence of neutrino oscillations driven by non-zero neutrino masses and neutrino mixing. Evidences for oscillations of neutrinos were obtained also in the first long baseline accelerator neutrino experiment K2K [8].

The recent Super-Kamiokande data on the $L=E$ -dependence of multi-GeV-like atmospheric neutrino events [6], L and E being the distance traveled by neutrinos and the neutrino energy, and the new more precise spectrum data of KamLAND and K2K experiments [9, 10], are the latest significant contributions to this progress. For the first time the data exhibit directly the effects of the oscillatory dependence on $L=E$ and E of the probabilities of oscillations in vacuum [11]. We begin to "see" the oscillations of neutrinos. As a result of these significant developments, the oscillations of solar e , atmospheric and μ , accelerator (at $L = 250$ km) and reactor e (at $L = 180$ km), driven by nonzero masses and mixing, can be considered as practically established.

The SK atmospheric neutrino and K2K data are best described in terms of dominant 2-neutrino ! (!) vacuum oscillations. The best fit values and the 99.73% C.L. allowed ranges of the atmospheric neutrino oscillation parameters $\sin^2 2\theta_{23} = \sin^2 2\theta_{31}$ and $\sin^2 2\theta_{13}$ read [6]: $\sin^2 2\theta_{31} = 2.1 \pm 10^{-3}$ eV 2 , $\sin^2 2\theta_{23} = 1.0$, $\sin^2 2\theta_{13} = (1.3 \pm 4.2) \times 10^{-3}$ eV 2 , $\sin^2 2\theta_{13} = 0.85$. The sign of $\sin^2 2\theta_{31}$ and of $\cos 2\theta_{23}$, if $\sin^2 2\theta_{23} \neq 1.0$, cannot be determined using the existing data.

The combined 2-neutrino oscillation analysis of the solar neutrino and the new KamLAND 766.3 Ty spectrum data shows [9, 12, 13] that the solar neutrino oscillation parameters lie in the low-LMA region: $\sin^2 2\theta_{13} = (7.9^{+0.6}_{-0.5}) \times 10^{-5}$ eV 2 , $\tan^2 \theta_{12} = (0.40^{+0.09}_{-0.07})$ [9]. The high-LMA solution is excluded at more than 3 σ . The value of $\sin^2 2\theta_{13}$ is determined with a remarkably high precision of 12% at 3 σ . Maximum solar neutrino mixing is ruled out at 6 σ .

The solar and atmospheric neutrino, and KamLAND and K2K neutrino oscillation data require the existence of three-neutrino mixing in the weak charged lepton current. In this case the neutrino mixing is characterised by one additional mixing angle θ_{13} (the only small mixing angle in the PMNS matrix). Three-neutrino oscillation analyses of the solar, atmospheric and reactor neutrino data show that $\sin^2 \theta_{13} < 0.05$ [12, 13]¹.

Understanding the origin of the patterns of solar and atmospheric neutrino mixing and of $\sin^2 2\theta_{21}$ and $\sin^2 2\theta_{31}$, suggested by the data, is one of the central problems in neutrino physics today. A prerequisite for any progress in our understanding of neutrino mixing is the knowledge of the precise values of solar and atmospheric neutrino oscillation parameters, θ_{12} , $\sin^2 2\theta_{21}$, and $\sin^2 2\theta_{23}$, $\sin^2 2\theta_{13}$ and of θ_{13} . In the present article we discuss the possibilities of high precision measurement of the solar neutrino mixing angle θ_{12} in solar and reactor neutrino experiments.

The solar neutrino mixing parameter $\sin^2 \theta_{12}$ is determined by the current KamLAND and solar neutrino data with a relatively large uncertainty of 24% at 3 σ . In the future, more precise spectrum data from the KamLAND experiment can lead to even more accurate determination of the value

¹After the new background data published by the KamLAND collaboration [27] the bound changes to $\sin^2 \theta_{13} < 0.055$ [12].

of m_{21}^2 . However, these data will not provide a considerably more precise measurement of \sin^2_{12} owing to the fact that the baseline of the KamLAND experiment effectively corresponds to a ν_e Survival Probability MAXimum (SPM MAX) [14, 15]. The analysis of the global solar neutrino data taking into account a possible reduction of the errors in the data from the phase-III of the SNO experiment shows that the uncertainty in the value of \sin^2_{12} would still remain well above 15% at 3 [17].

We begin by summarising the results on \sin^2_{12} , obtained using the current global solar and reactor neutrino oscillation data (section 2). We consider the improvements in the determination of \sin^2_{12} , which can be achieved with the expected increase of statistics and reduction of systematic errors in the experiments which are currently operating. In particular, the effect of KamLAND data, corresponding to a statistics of 3 kT_y, as well as of the data of phase-III of SNO experiment, are analysed.

We turn next to future experiments. We discuss first (in section 3) the possibility of high precision determination of \sin^2_{12} in a LowNu solar neutrino experiment, designed to measure the MeV and sub-MeV components of the solar neutrino flux: pp, pep, CNO, ^7Be . It is usually suggested that the LowNu experiments can provide one of the most precise measurements of the solar neutrino mixing angle [18, 19, 20]. Detailed analysis was carried out in [21] and it was concluded that a future pp experiment should have accuracy better than 3% in order to improve on the knowledge of \tan^2_{12} .

We consider a generic ν_e scattering experiment measuring the pp neutrino flux and perform a detailed quantitative analysis of the precision with which \sin^2_{12} can be determined in such an experiment. We examine the effect of including different representative values of the pp neutrino induced event rate in the χ^2 analysis of the global solar neutrino data. Three values (0.68, 0.72, 0.77) of the (normalized) event rate from the currently allowed 3 range are considered. The error in the measured rate is varied from 1% to 5%. We investigate how much the accuracy on \sin^2_{12} improves by adding the pp flux data in the analysis. The dependence of the sensitivity to \sin^2_{12} on the central value of the measured pp flux as well as on the measurement errors is studied. We compare the precision in \sin^2_{12} expected with assumed data on pp neutrinos included in the analysis, with the sensitivity that can be achieved using prospective results from phase-III of SNO experiment and 3 kT_y KamLAND data, and comment on the minimum error required in the LowNu pp experiments to improve the precision of \sin^2_{12} measurement. The impact of the uncertainty due to m_{13} on the allowed ranges of \sin^2_{12} is studied as well.

In the section 4 we analyse in detail the possibility of a high precision determination of \sin^2_{12} in a reactor experiment with a baseline of $L = (50 - 70)$ km, corresponding to a ν_e Survival Probability MINimum (SPM MIN). That such an experiment can provide the highest precision in the measurement of \sin^2_{12} was pointed out first in [14]. A rather detailed study of the precision in \sin^2_{12} , which might be achieved in an SPM MIN experiment with the flux of ν_e from the Kashiwazaki reactor complex in Japan and $L = 54$ km, was performed recently in [16]². We consider a generic SPM MIN reactor experiment with a KamLAND-type detector. We investigate the dependence of the precision on \sin^2_{12} which can be achieved in such an experiment on the baseline, statistics and systematic errors. More specifically, the spectrum data is simulated for

²In ref. [16] this experiment is called SADO.

four different true values of m_{21}^2 and for each of these values the optimal baseline at which the most precise measurement of \sin^2_{12} could be performed is determined. We show, in particular, that an independent determination of m_{21}^2 with sufficiently high accuracy would allow \sin^2_{12} to be measured with the highest precision over a relatively wide range of baselines. The effect of \sin^2_{13} uncertainty on the \sin^2_{12} determination is investigated in detail.

The results of the present study are summarized in section 5.

2 Measuring \sin^2_{12} in Existing Experiments

In this section we review the precision of m_{21}^2 and \sin^2_{12} determination from the existing solar neutrino and KamLAND data from two-neutrino oscillation analysis. We also discuss possible improvements in the precision that can be achieved in the currently running experiments.

2.1 Current Solar and Reactor Neutrino Data on \sin^2_{12}

In the present global solar neutrino and KamLAND data analysis we include

data from the radiochemical experiments, Cl [1] and Ga (Gallex, SAGE and GNO combined) [2],

the 1496 day 44 bin Zenith angle spectrum data from SK [3],

the 34 bin combined CC, NC and Electron Scattering (ES) energy spectrum data from the phase I (pure D_{20} phase) of SNO [4],

the data on CC, NC and ES total observed rates from the phase II (salt phase) of SNO experiment [5].

The 8B flux normalization factor f_B is left to vary freely in the analysis, while for the pp, pep, 7Be , ${}^{13}NO$, and hep fluxes the predictions and uncertainties from the recent standard solar model (SSM) [22] (BP04) are used. We skip the details of the χ^2 analysis, which can be found in [23, 24, 25].

We include the 766.3 Ty KamLAND data in the global analysis. For treatment of the latest KamLAND data in the combined analysis we refer the reader to [12], while details regarding the future-projected analysis with simulated KamLAND data are given in [26]. The best-fit in the combined analysis of solar and KamLAND data is obtained for [12]³

$$m_{21}^2 = 8.4 \times 10^{-5} \text{ eV}^2, \quad \sin^2_{12} = 0.28, \quad f_B = 0.88$$

In Fig. 1 we plot $\chi^2 = \chi^2_{\text{min}}$ as a function of m_{21}^2 (right panel) and \sin^2_{12} (left panel), for a two-neutrino oscillation fit of the global solar neutrino + KamLAND data. The parameters not given in each of the two panels are allowed to vary freely. From this figure one can easily read

³With the inclusion of the new KamLAND background data [27], the best-fit shifts to slightly smaller values of m_{21}^2 : $m_{21}^2 = 8.0 \times 10^{-5} \text{ eV}^2, \quad \sin^2_{12} = 0.28, \quad f_B = 0.88$ [12].

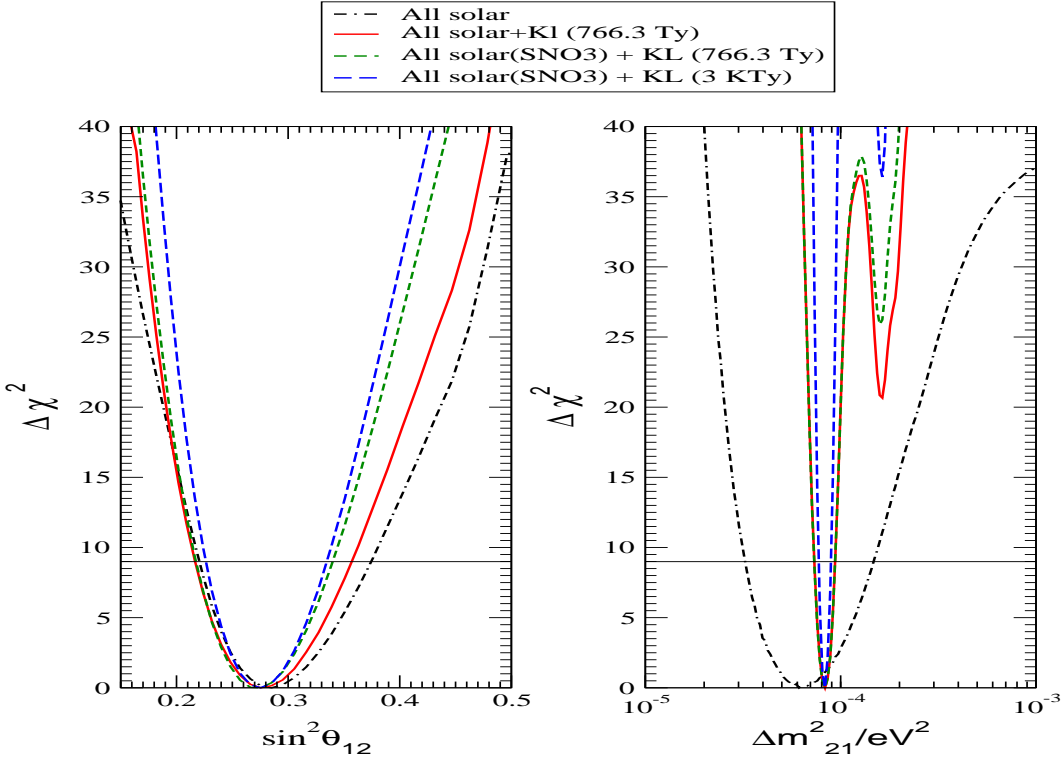


Figure 1: $\Delta\chi^2$ as a function of $\sin^2 \theta_{12}$ (left panel) and of m_{21}^2 (right panel). The curves shown are obtained from global analysis of the current solar neutrino data (black dot-dashed line), current solar + KamLAND data (red solid line), solar neutrino data with projected SNO-III errors + current KamLAND data (green short dashed line) and the solar neutrino data with projected SNO-III errors + prospective 3 kTy KamLAND data (blue long dashed line). The horizontal lines indicate the 3-sigma limit ($\Delta\chi^2 = 9$) for 1 parameter.

o the allowed ranges of the displayed parameter at various confidence levels. The horizontal line shows the 3-sigma limit corresponding to $\Delta\chi^2 = 9$ for a 1 parameter fit. In Table 1 we present the current 3-sigma allowed ranges of m_{21}^2 and $\sin^2 \theta_{12}$ obtained from Fig. 1. We also give the spread in these parameters which is defined as

$$\text{spread} = \frac{\text{prm}_{\text{max}} - \text{prm}_{\text{min}}}{\text{prm}_{\text{max}} + \text{prm}_{\text{min}}} \times 100 \quad (1)$$

where prm is either m_{21}^2 or $\sin^2 \theta_{12}$. Table 1 and Fig. 1 demonstrate clearly that the KamLAND experiment has remarkable sensitivity to m_{21}^2 . The inclusion of KamLAND data with increasing statistics in the analysis progressively reduces the spread in m_{21}^2 , and with the latest data the 3-sigma spread is 12%. This demonstrates, in particular, the extraordinary precision that has already been achieved in the determination of m_{21}^2 . On the other hand, the spread in $\sin^2 \theta_{12}$ is seen to be controlled mainly by the solar neutrino data and does not show any marked reduction

with the inclusion of the KamLAND data in the analysis. Using the global solar neutrino and KamLAND data allows to determine $\sin^2 \theta_{12}$ with an error of 24% at 3 σ .

2.2 Prospective KamLAND and SNO Data and $\sin^2 \theta_{12}$

We will analyze next the expected impact of future data from KamLAND and SNO experiments on the m_{21}^2 and $\sin^2 \theta_{12}$ determination.

The SNO experiment is sensitive to the flux of ${}^8\text{B}$ neutrinos with energy $E > 5 \text{ MeV}$. For the oscillation parameters in the low-LMA region, the ${}^8\text{B}$ neutrino survival probability of interest is given approximately by (MSW adiabatic transition probability):

$$P_{ee}({}^8\text{B}) \propto \sin^2 \theta_{12} : \quad (2)$$

The CC/NC ratio measured in SNO determines P_{ee} independently of the ${}^8\text{B}$ neutrino flux normalization. Thus, it can give a direct measure of $\sin^2 \theta_{12}$. Reducing the errors ($R_{CC} = R_{NC}$) in the measured CC and NC event rates in SNO, R_{CC} and R_{NC} , can improve the precision of determination of this parameter since

$$(\sin^2 \theta_{12}) = (R_{CC} = R_{NC}) : \quad (3)$$

The oscillations of reactor e detected in KamLAND experiment are practically not affected by Earth matter effects and the corresponding e survival probability has the form

$$P_{ee}^{KL} \propto 1 - \sin^2 2 \theta_{12} \sin^2 \frac{m_{21}^2 L}{4E} : \quad (4)$$

The average energy and baseline for KamLAND correspond to $\sin^2(m_{21}^2 L/4E) = 0$, i.e., to a Survival Probability Maximum (SPMAX). As a consequence, the coefficient of the $\sin^2 2 \theta_{12}$ term in P_{ee}^{KL} is relatively small, weakening the sensitivity of KamLAND to θ_{12} . As was shown in [4], the most precise measurement of $\sin^2 \theta_{12}$ can be performed in a reactor experiment with a baseline tuned to a Survival Probability Minimum (SPMIN), i.e., to $\sin^2(m_{21}^2 L/4E) = 1$. We will discuss the sensitivity to $\sin^2 \theta_{12}$, which can be achieved in such an experiment, in section 4.

In phase-III of the SNO experiment, the NC events will be observed directly (and independently from the CC events) using ${}^3\text{He}$ proportional counters. This will help to increase the NC statistics and reduce the systematic errors in the NC data. In addition, the correlations between the errors in the measured CC and NC event rates will be absent. The total projected error in the measured NC event rate in phase-III of SNO experiment is 6% [28]. We incorporate this in our analysis instead of the present error in R_{NC} of 9%. For the CC event rate R_{CC} measured at SNO we assume a somewhat reduced total error of 5%. We assume also that the central values of the measured CC and NC event rates will remain unchanged. The results of our analysis are shown in Fig. 1. The short dashed lines in Fig. 1 display the behavior of $\sin^2 \theta_{12}$ with anticipated SNO phase-III results and the reduced projected errors added to the global solar neutrino and KamLAND 766.3 Ty spectrum data. The figure shows that with the inclusion of the SNO phase-III prospective results, the allowed range of m_{21}^2 in the low-LMA region remains unchanged: it is determined

principally by the KamLAND data. However, the higher m_{21}^2 regions get more disfavored as the reduced errors in R_{CC} and R_{NC} lead to a stronger rejection of larger values of $R_{CC} = R_{NC}$ [29]. The figure also shows that the allowed range of $\sin^2 \theta_{12}$ gets further constrained from above. From Table 1 we see that the 3 spread of $\sin^2 \theta_{12}$ becomes 21% with the inclusion of projected SNO phase-III data in the presently existing set of data.

We also studied the effect of increased statistics of KamLAND experiment on the $\sin^2 \theta_{12}$ and m_{21}^2 determination. To this end, we include 3 kT y KamLAND spectrum data, simulated at $m_{21}^2 = 8.3 \times 10^{-5} \text{ eV}^2$, in our analysis with projected SNO phase-III data. We use a systematic error of 5% for KamLAND since the KamLAND systematic error is expected to diminish after the planned fiducial volume calibration and re-evaluation of the uncertainties in the power of the relevant nuclear stations. If the real KamLAND spectrum data conforms to this projected spectrum, the allowed range of m_{21}^2 would be further constrained, allowing the determination of m_{21}^2 with an accuracy of about 5%. The higher m_{21}^2 regions would be disfavored even stronger. The uncertainty in the value of $\sin^2 \theta_{12}$ would be smaller and the 3 spread, as seen from Table 1, could be 18%. Clearly, the uncertainty in $\sin^2 \theta_{12}$ cannot be reduced to 15% or less (at 3) by future data from the currently operating solar and reactor neutrino experiments.

Data set used	(3) Range of $m_{21}^2 \text{ eV}^2$	(3) spread in m_{21}^2	(3) Range of $\sin^2 \theta_{12}$	(3) spread in $\sin^2 \theta_{12}$
only sol	3.3 – 15.3	65%	0.22 – 0.38	27%
sol+ 766.3 Ty KL	7.4 – 9.5	12%	0.22 – 0.36	24%
sol(+ SNO 3) + 766.3 Ty KL	7.4 – 9.5	12%	0.22 – 0.34	21%
sol(+ SNO 3)+ 3K Ty KL	7.7 – 8.9	7%	0.23 – 0.33	18%

Table 1: The 3 allowed ranges and spread (in per cent) of m_{21}^2 and $\sin^2 \theta_{12}$ obtained from 1 parameter fits.

3 Determining θ_{12} from Measurement of the pp Solar Neutrino Flux

The pp fusion reaction is the main contributor to the observed solar luminosity and the corresponding pp neutrinos constitute the largest and dominant component of the solar neutrino flux. The SSM uncertainty in the predicted solar neutrino fluxes is the least for the pp neutrinos (1%) [22]. So far only the Ga experiments have provided information on the pp neutrino flux because of their low energy threshold of 0.23 MeV. Sub-MeV solar neutrino experiments (LowNu experiments) are being planned for measuring the flux of pp neutrinos using either charged current reactions (LENS, MOON, SIREN) or e elastic scattering (XMASS, CLEAN, HERON, MUNU, GENIUS) [18, 19, 20]. Since according to the SSM, most of the energy released by the Sun (99%) is generated in the pp cycle of reactions in which also the pp neutrinos are produced, a precise determination of the pp neutrino flux would lead to a better understanding of the solar energetics

and, more generally, of the physics of the Sun. It has also been realized that high precision measurement of the pp neutrino flux can be instrumental for more accurate determination of the solar neutrino mixing parameter, which, as we have seen in the preceding section, will not be determined with an uncertainty smaller than 18% (at 3 σ) by the currently operating experiments.

Since the pp neutrino energy spectrum extends up to 0.42 MeV only, for m_{21}^2 in the LMA region, the pp neutrino oscillations are practically not affected by matter effects in the Sun or the Earth. Thus, to a good approximation, the pp neutrino oscillations are described by the survival probability in the case of oscillations in vacuum, in which the oscillating term is strongly suppressed by the averaging over the region of neutrino production in the Sun [30]:

$$P_{ee}^2(pp) = 1 - \frac{1}{2} \sin^2 2\pi_{12}; \quad (5)$$

The normalized event rate for a e scattering (ES) and charged current (CC) experiments measuring the pp neutrino flux is given respectively by

$$R_{pp} = hP_{ee}^2(pp)i + r_{pp}(1 - hP_{ee}^2(pp)i) \text{ for ES experiments;} \quad (6)$$

$$R_{pp} = hP_{ee}^2(pp)i \text{ for CC experiments;}, \quad (7)$$

where $r_{pp} = 0.3$ and $h \cdot i$ denotes averaged probabilities. For an ES experiment, the second term in eq. (6) represents the NC contribution. Since the pp neutrino survival probability is largely independent of energy one can use eq. 5 for the averaged probabilities. Using eqs. (5) – (7), one finds for the uncertainty in $\sin^2 2\pi_{12}$ determination:

$$(\sin^2 2\pi_{12})_{pp}^{CC} = \frac{R_{pp}}{2 \cos 2\pi_{12}} \text{ for CC experiments} \quad (8)$$

$$(\sin^2 2\pi_{12})_{pp}^{ES} = \frac{R_{pp}}{2 \cos 2\pi_{12}} \frac{1}{1 - r_{pp}} \text{ for ES experiments} \quad (9)$$

where R_{pp} is the error in the measured value of R_{pp} . A comparison of eq. (8) with eq. (3) shows that for the same value of R_{pp} and of the error in the CC to NC event rate ratio measured by SNO, ($R_{CC} = R_{NC}$), the pp neutrino experiments of the CC type can provide a more precise measurement of $\sin^2 2\pi_{12}$ only if $\cos 2\pi_{12} > 0.5$ ($\sin^2 2\pi_{12} < 0.25$). Similarly, it follows from eq. (9) and eq. (3) that for $R_{pp} = (R_{CC} = R_{NC})$, the ES pp experiment could provide a more precise determination of $\sin^2 2\pi_{12}$ only if the true value of $\cos 2\pi_{12} > 0.71$ ($\sin^2 2\pi_{12} < 0.14$). Since the currently allowed 3 σ range of $\sin^2 2\pi_{12}$ is $\sin^2 2\pi_{12} = (0.22 \pm 0.38)$, for almost all of the allowed values of $\sin^2 2\pi_{12}$, SNO will have a better sensitivity to $\sin^2 2\pi_{12}$ than a LowNu pp experiment measuring the pp neutrino flux with the same experimental error as the error in the SNO data on the ratio $R_{CC} = R_{NC}$.

In order to improve the accuracy of $\sin^2 2\pi_{12}$ determination after the SNO phase-III results will be available, the total experimental error in the measured event rate in the pp experiments has to be sufficiently small, which requires high statistics and well understood systematics. In the present section we will quantify these statements by incorporating hypothetical data on the pp

neutrino ux in our analysis. We consider a generic pp neutrino ES experiment⁴ and consider some illustrative sample rates from the currently predicted range. We give quantitative estimate of the sensitivity to $\sin^2 \theta_{12}$ expected to be achieved in i) a pp experiment, and ii) combining the prospective data from a pp experiment with the global solar and reactor neutrino data. In particular, we estimate the maximum error in a pp ux measurement, for which the uncertainty in the determined value of $\sin^2 \theta_{12}$ would be smaller than that expected after the inclusion of the SNO phase-III results. We use in this analysis the pp neutrino ux and its 1% uncertainty predicted by the BP04 SSM [22]. The 1% error due to SSM uncertainties is added to the experimental errors in the pp ux determination.

3.1 Two Generation Analysis

We consider a generic e scattering experiment which can measure the pp neutrino ux. The experiment is assumed to have a kinetic energy threshold of 50 keV. We suppose that the BP04 SSM predicts correctly the pp ux. The predicted event rate ("pp rate") in such an experiment for the best t values of the oscillation parameters, normalized to the rate predicted by the BP04 model in the absence of neutrino oscillations, is 0.71; the predicted 3 range for the normalized pp rate is 0.67–0.76 [12]. We will consider three illustrative values of the normalized pp rate, 0.68, 0.72 and 0.77, and vary the experimental error in the measured pp rate from 1% to 5%. The estimated theoretical uncertainties due to the SSM and their correlations for the pp neutrino ux are included in the analysis following the standard covariance approach [31]. Thus, we minimize the χ^2 defined as

$$\chi^2 = \sum_{i,j=1}^N (R_i^{\text{expt}} - R_i^{\text{theory}})^2 (R_{ij}^2)^{-1} (R_j^{\text{expt}} - R_j^{\text{theory}})^2 \quad (10)$$

where R_i are the solar neutrino data points, N is the number of data points and $(R_{ij}^2)^{-1}$ is the inverse of the covariance matrix, containing the squares of the correlated and uncorrelated experimental and theoretical errors. The ${}^8\text{B}$ ux normalization factor f_B is left to vary freely in the analysis. The errors and correlations due to the other uxes are taken from the BP04 SSM⁵.

Let us begin by analysing first the potential results from a possible future pp neutrino experiment alone. In this case eq. (6) can be used to get the approximate values of $\sin^2 \theta_{12}$ for a given pp rate,

$$\sin^2 \theta_{12} = \frac{2(1 - R_{\text{pp}})}{1 + R_{\text{pp}}} : \quad (11)$$

If we assume a pp rate of 0.72 and 1% experimental error (in addition to the SSM uncertainty of 1%), the χ^2 analysis gives for the 3 range of allowed values of $\sin^2 \theta_{12}$ $0.21 < \sin^2 \theta_{12} < 0.33$. This

⁴A comparison of eqs. (8) and (9) shows that the CC pp experiments could achieve a better sensitivity on $\sin^2 \theta_{12}$ due to the absence of the 30% "contamination" caused by the NC events present in the ES event sample. In what follows, we present results for an ES pp neutrino experiment (XMASS, etc.). Henceforth the term "pp" experiment implies an ES pp neutrino experiment.

⁵One can also keep the normalization of the pp neutrino ux as a variable parameter, subject to the solar luminosity constraint [21].

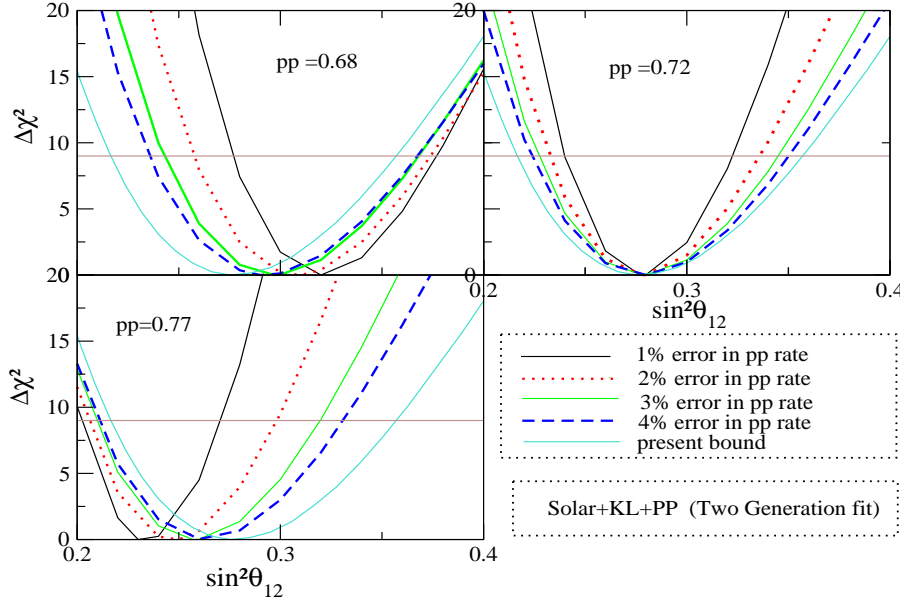


Figure 2: χ^2 as a function of $\sin^2 \theta_{12}$. The results shown are obtained in a two-neutrino oscillation analysis of the global solar neutrino and KamLAND 766.3 Ty spectrum data and simulated data from a LowNu pp neutrino experiment. The three panels correspond to three illustrative values of the event rate due to pp neutrinos in the LowNu experiment ("pp rate"), normalized to the rate predicted by the BP04 SSM. In each case results for four different assumed values of the error in the measured pp rate are shown. We also show the curve obtained in global analysis of the current solar and reactor neutrino data. The horizontal line indicates the 3 σ limit ($\chi^2 = 9$) for 1 parameter t .

agrees very well with what one would obtain using eq. (11) including the errors along with the mean pp rate value of 0.72. Thus, the spread in $\sin^2 \theta_{12}$ is of about 22%, which is not much smaller than the spread in $\sin^2 \theta_{12}$ determined using the current data. In what follows, we will perform an analysis of the data from all experiments, including illustrative rates from a e scattering type pp experiment, when estimating the sensitivity to the mixing angle θ_{12} .

Figures 2 and 3 show results obtained in a two-neutrino oscillation analysis of the KamLAND and global solar neutrino data, including the pp rate assumed to be measured in the LowNu ES experiment. In Fig. 2 we plot the dependence of χ^2 on $\sin^2 \theta_{12}$ and show results for four values of the error in the measured pp rate, 1%, 2%, 3% and 4%. The cyan colored lines correspond to results obtained using the currently existing data. One can easily read from the figure the range of allowed values of $\sin^2 \theta_{12}$ at a given C.L. for a chosen experimental error in the pp rate measurement. In Fig. 3 the corresponding allowed range of $\sin^2 \theta_{12}$ is shown as a function of the error in the pp rate measurement. We let the pp rate error vary from 1% to 5%. The various bands

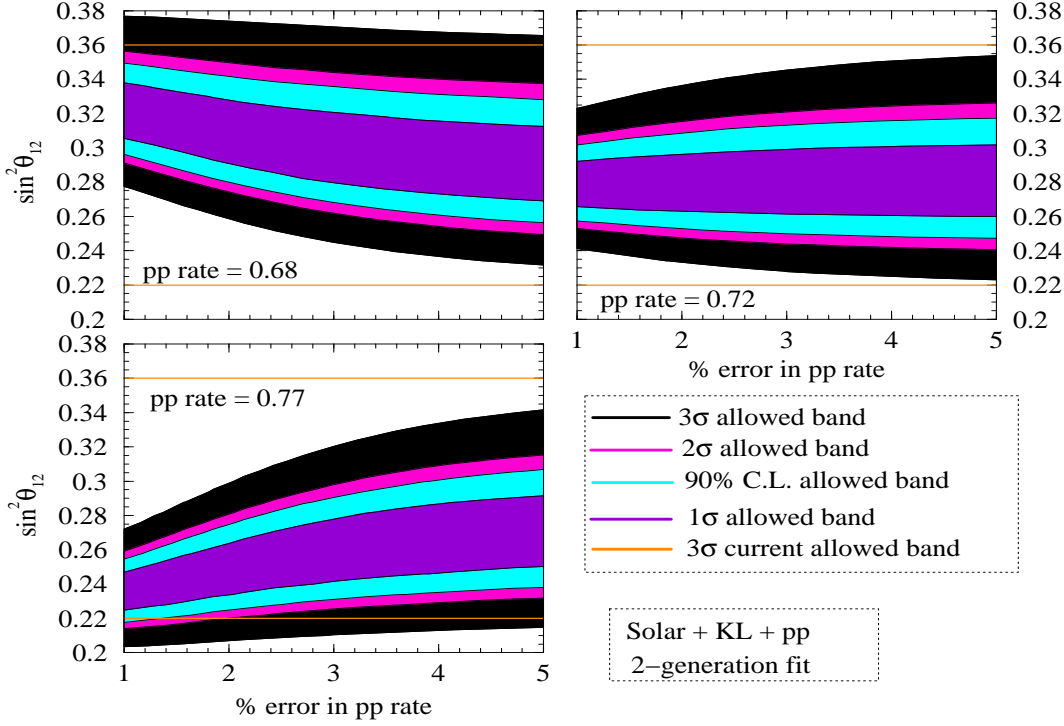


Figure 3: The 1 (68.27% C.L.), 1.64 (90% C.L.), 2 (95.45% C.L.) and 3 (99.73% C.L.) allowed range of $\sin^2 \theta_{12}$ as a continuous function of the error in the pp rate for three assumed mean values of the measured pp rate. Shown is also the current 3 allowed range of $\sin^2 \theta_{12}$.

correspond to 68.27% C.L. (1), 90% C.L. (1.64), 95.45% C.L. (2) and 99.73% C.L. (3). For comparison, the 3 range of the presently allowed values of $\sin^2 \theta_{12}$ is indicated in the figure by horizontal lines.

In both figures we present results for the 3 assumed values of the measured pp rate, R_{pp} . The figures show that:

1. For $R_{pp} = 0.68$ at the lower end of the predicted range of values of the pp rate, the lower bound on $\sin^2 \theta_{12}$ increases considerably with reducing the error in the pp flux measurement. The upper bound also increases but not significantly: the reduction of the error in pp rate measurement has a much smaller effect on the maximal allowed value of $\sin^2 \theta_{12}$.
2. For $R_{pp} = 0.72$, which is close to the best-predicted rate, both the lower bound on $\sin^2 \theta_{12}$ increases and the upper bound decreases, tightening the allowed range of $\sin^2 \theta_{12}$. Reducing the error in the pp flux measurement improves the precision of determination of $\sin^2 \theta_{12}$.
3. For the relatively high pp rate, $R_{pp} = 0.77$, the minimal allowed value of $\sin^2 \theta_{12}$ diminishes somewhat, while the maximal allowed value diminishes considerably.

These features can be understood by analyzing the expression for the probability of survival of pp neutrinos given in eq. (6). It is evident that a lower pp rate drives $\sin^2 \theta_{12}$ towards higher

values and vice versa. Therefore the lower bound on $\sin^2 \theta_{12}$ increases for $R_{pp} = 0.68$. The effect of reducing the error in the pp flux measurement has the effect of pushing θ_{12} towards higher values. Likewise, one could expect that the maximal value of $\sin^2 \theta_{12}$ should equally increase for $R_{pp} = 0.68$. However, since we have used the global solar neutrino data in the analysis, the maximal allowed value of $\sin^2 \theta_{12}$ increases only slightly as the corresponding higher values of $\sin^2 \theta_{12}$ are strongly disfavored by the already existing data. Thus, if a future pp (ES) experiment measures a value of R_{pp} near the lower end of the presently predicted range, the lower limit on $\sin^2 \theta_{12}$ will increase as the error in the measured R_{pp} is reduced. The upper limit will increase slightly, but the effect of reducing the pp rate error will not be drastic.

A higher measured value of R_{pp} , $R_{pp} = 0.77$, requires a lower value of $\sin^2 \theta_{12}$. Consequently, the maximal allowed value of $\sin^2 \theta_{12}$ is seen to diminish substantially. The lower limit on $\sin^2 \theta_{12}$ could be pushed to relatively small values by the data from the pp experiment alone. However, such small values of $\sin^2 \theta_{12}$ are already excluded by the current set of data and therefore the lower limit on $\sin^2 \theta_{12}$ cannot reduce much.

A pp rate of $R_{pp} = 0.72$ is quite consistent with the current best-fit values of the parameters. As a consequence, the corresponding maximal allowed value of $\sin^2 \theta_{12}$ diminishes and the minimal value increases as the error in R_{pp} is reduced. Thus, the precision of $\sin^2 \theta_{12}$ determination increases.

We summarize in Table 2 (columns 3 and 4) the range of allowed values of $\sin^2 \theta_{12}$ expected from a combined analysis of KamiLAND and global solar neutrino data and the future (hypothetical) data from the pp experiment. With a 1% experimental error in the pp rate, the 3-sigma spread can decrease to about 14%. We note that the maximal and/or minimal allowed values of $\sin^2 \theta_{12}$ depend critically on the measured mean value of the pp rate. However, the spread in $\sin^2 \theta_{12}$ is practically independent of the latter. For $R_{pp} = 0.72$, the 3-sigma spread in the value of $\sin^2 \theta_{12}$ is approximately 23%, 19%, 18% and 14% respectively for an error in the pp rate of 4%, 3%, 2% and 1% (Table 2, 4th column). The 3-sigma spread in $\sin^2 \theta_{12}$ after including the phase-III SNO data would be about 21% (Table 1). We observe that the error in the pp flux measurement should not exceed < 3% in order for the pp flux measurement to bring any further improvement in the precision of $\sin^2 \theta_{12}$ determination.

In Fig. 4 we show the expected range of allowed values of $\sin^2 \theta_{12}$ as a function of the error in the measured pp rate, after the potential results and projected errors from phase-III of the SNO experiment (SNO 3) are included in the global analysis. If the measured mean pp rate is 0.68 (0.77), the maximal (minimal) allowed value of $\sin^2 \theta_{12}$ slightly increases (decreases) and the minimal (maximal) value increases (decreases) significantly. The total uncertainty in $\sin^2 \theta_{12}$ is independent of the central value of the pp rate, in agreement, with what we have found earlier. For $R_{pp} = 0.72$, the 3-sigma spread in $\sin^2 \theta_{12}$ is 21%, 18%, 18%, 14% for a 4%, 3%, 2% and 1% experimental error in R_{pp} , respectively.

It follows from our analysis that the data from the pp experiment can allow to reduce the expected uncertainty of 21% in the determination of $\sin^2 \theta_{12}$ after the prospective phase-III SNO results are included in the analysis only if the error in the measured pp rate does not exceed 4%. However, even with $R_{pp} = 1\%$, the 3-sigma spread in the value of $\sin^2 \theta_{12}$ would not be smaller than 14%.

Table 2 summarizes the results on the allowed ranges and spread of $\sin^2 \theta_{12}$, obtained in a

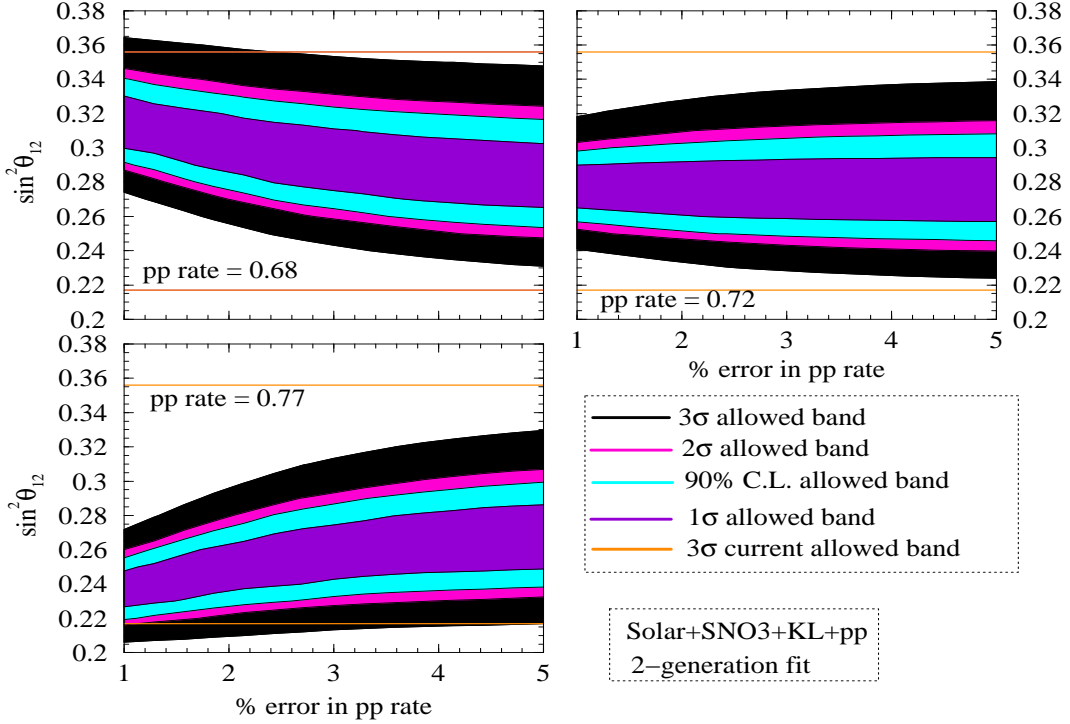


Figure 4: Same as Fig. 3 but including the prospective data (and errors) from the phase-III of SNO experiment.

two-neutrino oscillation analysis including SNO-III projected errors. As expected, the spread in $\sin^2 \theta_{12}$ reduces with inclusion of the phase-III SNO data in the analysis. Note that the ranges given in Table 2 are with the present KamLAND 766.3 Ty spectrum data. If we use future higher statistics data from KamLAND, the allowed spread in $\sin^2 \theta_{12}$ may reduce somewhat.

3.2 The Impact of N on-Zero 13

The solar and atmospheric neutrino, K2K and KamLAND data suggest the existence of 3-neutrino mixing and oscillations (see, e.g., [32]). Actually, all existing neutrino oscillation data, except the data of LSND experiment⁶ [34], can be described assuming 3-neutrino mixing. This warrants a 3-neutrino oscillation analysis of the potential sensitivity of a LowNupp neutrino experiment to $\sin^2 \theta_{12}$.

The 3-neutrino oscillations of interest are characterized by the neutrino mass-squared differences which drive the solar and atmospheric neutrino oscillations, $m_{21}^2 = m^2 > 0$ and $m_{31}^2 = m_{\text{atm}}^2$ respectively, and by the 3 mixing angles in the Pontecorvo-Maki-Nakagawa-Sakata (PMNS) neutrino mixing matrix, θ_{12} , θ_{23} and θ_{13} . In the standard parametrization of the PMNS matrix (see, e.g., [32]), the angles θ_{12} and θ_{23} coincide with the angles which control the

⁶In the LSND experiment indications for oscillations ! with $(m^2)_{\text{LSND}} < 1 \text{ eV}^2$ were obtained. The LSND results are being tested in the MiniBooNE experiment [35].

pp rate	% error	solar+ reactor + pp		solar(+ SN03)+ reactor+ pp	
		3 range	spread	3 range	spread
0.68	1	0.28 - 0.38	15.2%	0.27 - 0.36	14.3%
	2	0.26 - 0.37	17.5%	0.26 - 0.36	16.1%
	3	0.24 - 0.37	21.3%	0.24 - 0.35	18.6%
	4	0.24 - 0.37	21.3%	0.23 - 0.35	20.7%
0.72	1	0.24 - 0.32	14.3%	0.24 - 0.32	14.3%
	2	0.23 - 0.33	17.9%	0.23 - 0.32	16.4%
	3	0.23 - 0.34	19.3%	0.23 - 0.33	17.9%
	4	0.22 - 0.35	22.8%	0.22 - 0.34	21.4%
0.77	1	0.20 - 0.27	14.9%	0.20 - 0.27	14.9%
	2	0.21 - 0.30	17.6%	0.21 - 0.29	16.0%
	3	0.21 - 0.32	20.8%	0.21 - 0.31	19.2%
	4	0.21 - 0.33	22.2%	0.21 - 0.32	20.8%

Table 2: The 3 allowed ranges and % spread of $\sin^2 \theta_{12}$ obtained in a two-neutrino oscillation analysis of the solar neutrino data, including the simulated data on the pp neutrino flux, and the KamLAND 766.3 Ty spectrum data.

oscillations of solar and atm ospheric neutrinos, while θ_{13} is the angle limited by the data from the CHOOZ experiment. The precise limit on θ_{13} depends strongly on m_{atm}^2 (see e.g. [33]). The existing atm ospheric and reactor neutrino data imply [12, 13]

$$\sin^2 \theta_{13} < 0.05; \quad 99.73\% \text{ CL:} \quad (12)$$

The aim of the analysis which follows is to quantify the uncertainty which the absence of precise knowledge of the value of the CHOOZ angle θ_{13} introduces in the precision of $\sin^2 \theta_{12}$ determination.

The analyses of the latest SK atm ospheric neutrino and of the global solar neutrino data show also that [6, 12, 13] $m_{31}^2 \approx m_{\text{atm}}^2 \approx 2.1 \times 10^{-3} \text{ eV}^2$ and $m_{21}^2 = m^2 \approx 8 \times 10^{-5} \text{ eV}^2$. Thus, we have $m_{21}^2 \ll m_{31}^2$. Under this condition the probabilities of survival of the solar e and of the reactor e , relevant for the 3-neutrino oscillation interpretation of the solar neutrino and KamLAND data, have the form :

$$P_{ee}^3 = \cos^4 \theta_{13} P_{ee}^2 + \sin^4 \theta_{13} \quad (13)$$

where P_{ee}^2 is the corresponding probability of survival of e or e in the case of 2-neutrino mixing (see, e.g., [37]). For the reactor e detected at KamLAND, P_{ee}^2 is given by eq. (4). For solar neutrinos, P_{ee}^2 is the e survival probability in the case of 2-neutrino oscillation [38, 30] in which the solar electron number density N_e is replaced by $N_e \cos^2 \theta_{13}$. From eqs. (2), (5), (12) and (13) we get:

$$P_{ee}^3 ({}^8\text{B}) = \cos^4 \theta_{13} \sin^2 \theta_{12}; \quad (14)$$

$$P_{ee}^3 (\text{pp}) = \cos^4 \theta_{13} \left(1 - \frac{1}{2} \sin^2 2 \theta_{12}\right); \quad (15)$$

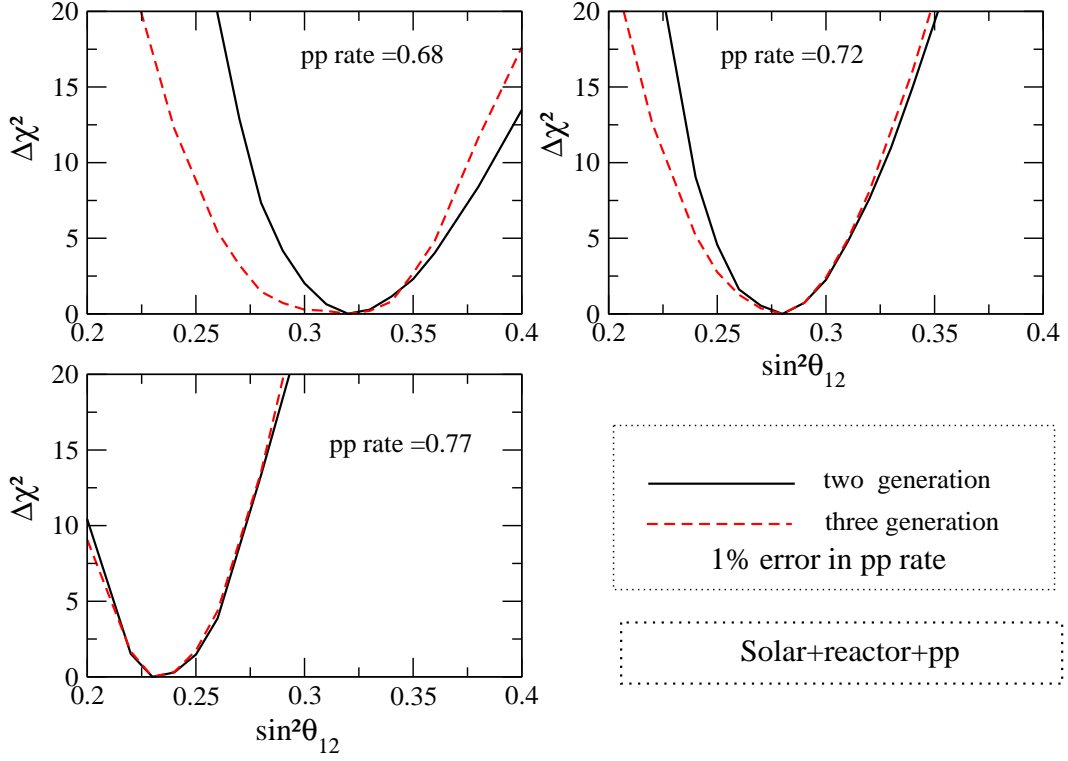


Figure 5: Comparison of $\Delta\chi^2$ vs. $\sin^2\theta_{12}$ obtained from a two generation analysis (solid black line) and three generation analysis (dashed red line) analyses of the world neutrino data including the pp rate. The three panels show the results for the three illustrative values of the pp rate. We present the results for 1% error in the pp rate. For the three-neutrino oscillation analysis $\sin^2\theta_{13}$ is allowed to vary freely, and for each case we present the plots for four different values of the % error in the pp rate.

Note that for a given value of P_{ee}^3 (pp), a non-zero value of θ_{13} decreases the measured value of θ_{12} , for the low energy pp flux. On the other hand, for a given value of P_{ee}^3 (8B), a non-zero θ_{13} increases the measured value of θ_{12} , for the higher energy 8B flux.

For $m_{21}^2 \ll jm_{31}^2$, the probability relevant for the interpretation of data from the CHOOZ experiment is given by

$$P_{ee\text{CHOOZ}}^3 = 1 - \sin^2 2\theta_{13} \sin^2(m_{31}^2 L/4E) : \quad (16)$$

Note that the probability $P_{ee\text{CHOOZ}}^3$ depends on m_{31}^2 , unlike the probabilities relevant for the interpretation of the solar and KamLAND data. In the analysis which we have performed jm_{31}^2 was allowed to vary freely within the 3 allowed range given in [6]⁷.

In Fig. 5 we show the dependence of $\Delta\chi^2$ on $\sin^2\theta_{12}$, obtained in a 3-neutrino oscillation analysis of the combined KamLAND, CHOOZ and solar neutrino data, including the simulated

⁷Details of our 3-neutrino oscillation analysis can be found in [39].

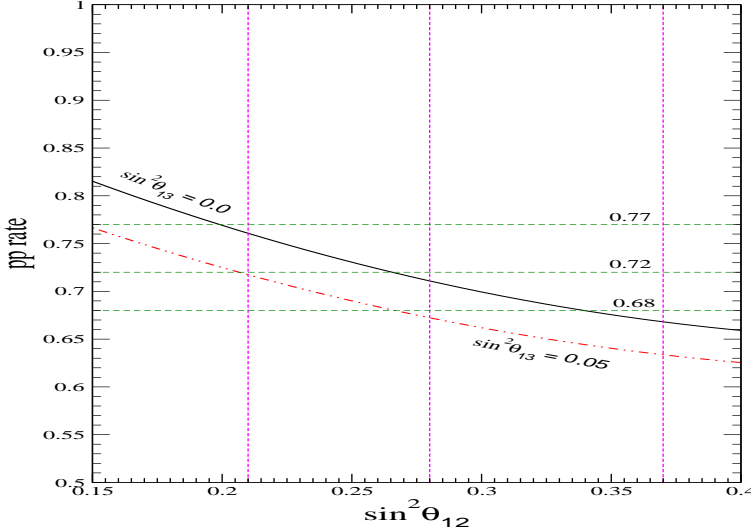


Figure 6: The pp rate as a function of $\sin^2 \theta_{12}$. The black solid line is the pp rate for $\sin^2 \theta_{13} = 0$ while the red dot-dashed line is $\sin^2 \theta_{13} = 0.05$. We also show our illustrative pp rates of 0.68, 0.72 and 0.77 on the plot.

data on the pp neutrino flux. The results shown are for the three illustrative central values of R_{pp} considered earlier, and for the case of 1% error in R_{pp} . Except for $\sin^2 \theta_{12}$, all the other parameters, including $\sin^2 \theta_{13}$, were allowed to vary freely in the analysis. For comparison, results for $\sin^2 \theta_{13} = 0$ are shown in the same figure.

We find that

For a relatively low value of the measured pp rate, $R_{pp} = 0.68$, a non-zero $\sin^2 \theta_{13}$ leads to smaller minimum and maximum allowed values of $\sin^2 \theta_{12}$.

For $R_{pp} = 0.72$, the minimum allowed value of $\sin^2 \theta_{12}$ diminishes, while the maximum allowed value remains unaffected.

If $R_{pp} = 0.77$, both values are practically unaffected.

To help explain these features, we plot in Fig. 6 the pp rate (cf. Eqs. (6) and (15)) as a function of $\sin^2 \theta_{12}$ for $\sin^2 \theta_{13} = 0$ and $\sin^2 \theta_{13} = 0.05$. The three horizontal lines in the figure correspond to the three central values of R_{pp} considered in our analysis. We see from the figure that,

1. For a given value of $\sin^2 \theta_{12}$, a non-zero $\sin^2 \theta_{13}$ always reduces the predicted pp rate,
2. For a given measured pp rate, a non-zero $\sin^2 \theta_{13}$ would reduce the measured value of $\sin^2 \theta_{12}$,
3. For a given measured pp rate there is always a limiting value of $\sin^2 \theta_{12}$, such that for $\sin^2 \theta_{12}$ exceeding this value a non-zero $\sin^2 \theta_{13}$ does not affect the allowed values of $\sin^2 \theta_{12}$.

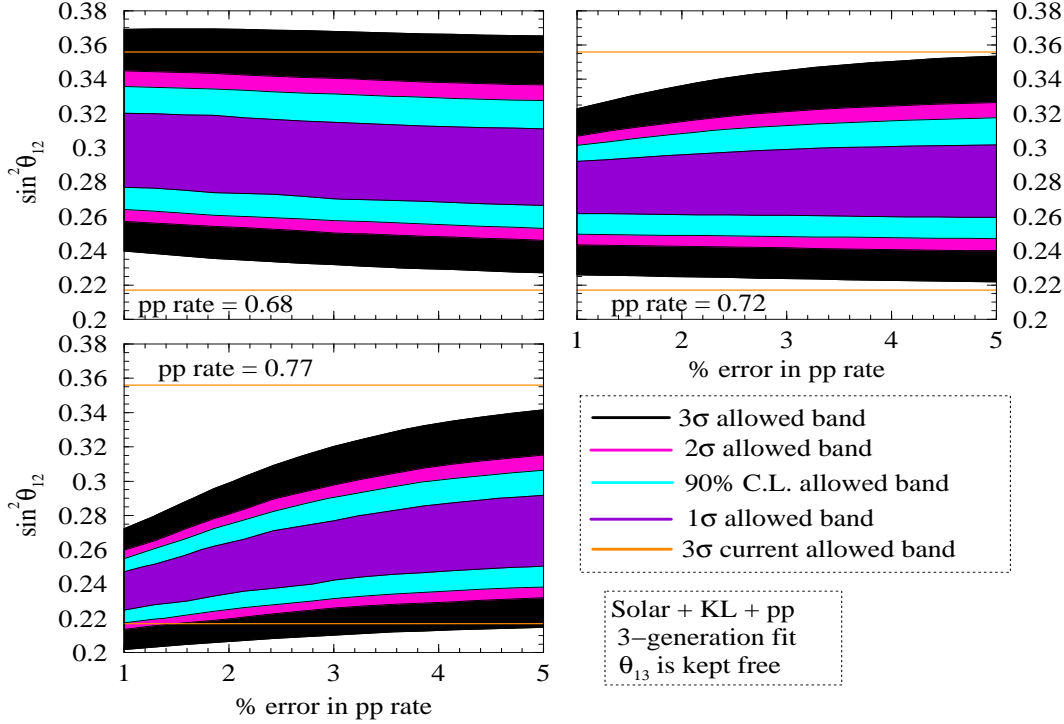


Figure 7: Same as Figure 3 but for a three generation analysis including all neutrino data and keeping $\sin^2 \theta_{13}$ free. We also show the 3 σ allowed band of $\sin^2 \theta_{12}$ from the current data.

Points (1) and (2) imply, in particular, that if for a given value of $\sin^2 \theta_{12}$ the pp rate predicted assuming 2-neutrino oscillations is larger than the measured pp rate, a non-zero θ_{13} can improve the quality of the fit. Thus, values of $\sin^2 \theta_{12}$ smaller than the minimal allowed one determined in a 2-neutrino oscillation analysis, could become allowed in the case of 3-neutrino oscillations due to non-zero $\sin^2 \theta_{13}$. As a consequence of point 3 we can conclude that if for a particular value of $\sin^2 \theta_{12}$, the pp rate predicted in the case of 2-neutrino oscillations is larger than the measured pp rate, a $\sin^2 \theta_{13}$ which differs from 0 substantially and further lowers the pp rate, would not be favored by the data. We use these features to explain Fig. 5. However it is to be borne in mind that Fig. 6 contains only the pp rates while in Figure 5 we show the results from a combined analysis of global solar and KamLAND data.

We see from Fig. 6 that the pp rate, predicted in the case of 2-neutrino oscillations, exceeds 0.72 for $\sin^2 \theta_{12} < 0.27$. Therefore in this case a non-zero $\sin^2 \theta_{13}$ improves the quality of the fit for all values of $\sin^2 \theta_{12} < 0.27$. Thus, relatively small values of $\sin^2 \theta_{12}$ which are disfavored by the 2-neutrino oscillation analysis, could become allowed if $\sin^2 \theta_{13} \neq 0$. This would lead to a smaller minimal allowed value of $\sin^2 \theta_{12}$. For $\sin^2 \theta_{12} > 0.27$, the predicted 2-neutrino oscillation rate is already lower than 0.72, and therefore a non-zero θ_{13} would not change the minimal allowed value of $\sin^2 \theta_{12}$.

The predicted R_{pp} for 2-neutrino oscillations can be greater than $R_{pp} = 0.77$ only for rela-

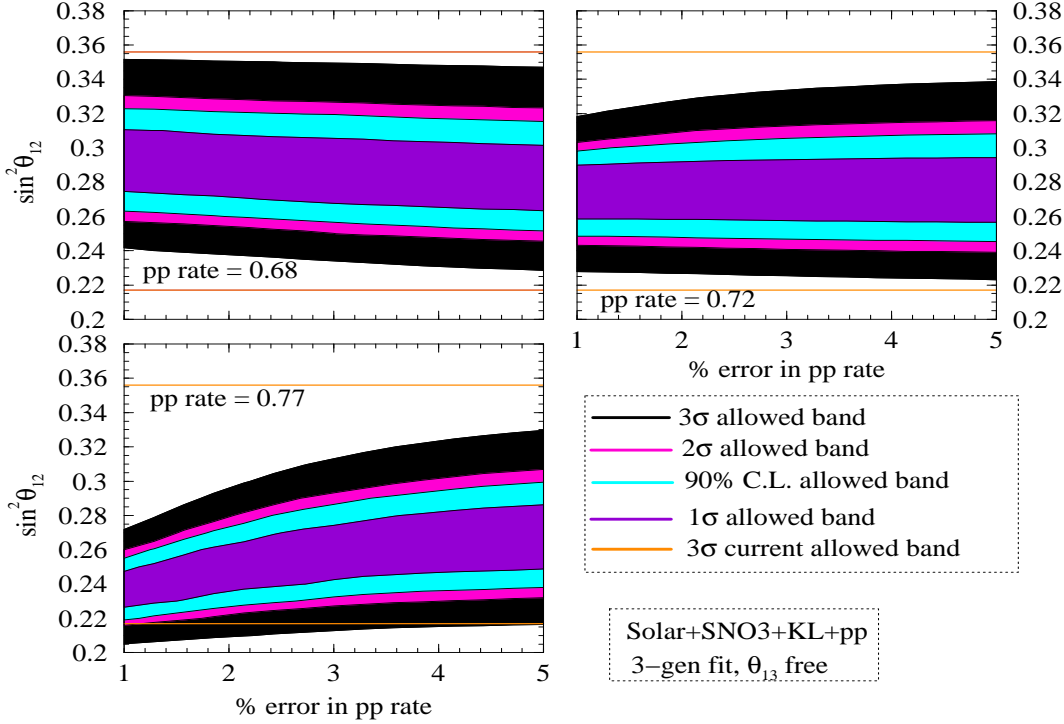


Figure 8: Same as Figure 7 but with the projected error from the third phase of the SNO experiment included. We show the 3-sigma allowed band from current data.

tively small values of $\sin^2 \theta_{12}$, which are strongly disfavored (if not ruled out) by the current data. Consequently, a non-zero $\sin^2 \theta_{13}$ is not expected to make any impact on the $\sin^2 \theta_{12}$ determination if the measured $R_{pp} = 0.77$.

In the case of a measured $R_{pp} = 0.68$, the predicted 2-neutrino oscillation pp rate is larger than 0.68 for $\sin^2 \theta_{12} < 0.34$ and a non-zero value of $\sin^2 \theta_{13}$ can improve the quality of the fit for a large range of values of $\sin^2 \theta_{12}$. This explains why the minimal allowed value of $\sin^2 \theta_{12}$ diminishes considerably for $\sin^2 \theta_{13} \neq 0$ in Fig. 5. The maximal allowed value of $\sin^2 \theta_{12}$ is also seen to reduce. The reason for this can be understood if one notes that the values of $\sin^2 \theta_{12}$ favoured by the pp experiment, for $\sin^2 \theta_{13} = 0$, would correspond to a relatively higher value of $R_{CC} = R_{NC}$ compared to that measured at SNO. If θ_{13} is non-zero, then the same R_{pp} could be produced at a lower value of θ_{12} . Since the predicted $R_{CC} = R_{NC}$ in SNO is given by Eq. (14), this lower $\sin^2 \theta_{12}$ coupled with non-zero θ_{13} would help reduce the 8B probability and the pp "data" could be "reconciled" with the SNO CC/NC data. Therefore for $R_{pp} = 0.68$, the best-fit from a three generation analysis comes at a non-zero value of $\sin^2 \theta_{13}$ and a lower value of $\sin^2 \theta_{12}$. Note that the value of the global χ^2_{min} for the three generation case ($\theta_{13} \neq 0$) is lower than the two-generation case ($\theta_{13} = 0$). However as noted before, since the predicted R_{pp} is already lower than 0.68 for $\sin^2 \theta_{12} > 0.34$, the pp experiment would force $\theta_{13} = 0$ for these high values of $\sin^2 \theta_{12}$. Thus above $\sin^2 \theta_{12} > 0.34$

the Δm^2 remains the same irrespective of whether $\sin^2 \theta_{13}$ was kept free (three-generation) or fixed at zero (two-generation). However, since the global Δm^2 was lower for the three-generation fit, the very high values of $\sin^2 \theta_{12}$, which were allowed in the two-generation analysis get disfavored by the three-generation fit.

In Fig. 7 we depict the $\sin^2 \theta_{12}$ sensitivity of the world neutrino oscillation data, including the sample data on the pp rate, as a function of % error in the measured pp rate in the case when $\sin^2 \theta_{13}$ is kept free. In Table 3 we give the corresponding 3 ranges of allowed values and spread of $\sin^2 \theta_{12}$ (columns 3 and 4). A comparison of this figure with Fig. 3 and the Table 3 with Table 2 demonstrates clearly all the specific features associated with the three values of the pp rate discussed above:

For $R_{pp} = 0.77$, $\sin^2 \theta_{13} \neq 0$ hardly makes any difference.

For $R_{pp} = 0.72$, the minimal allowed value of $\sin^2 \theta_{12}$ diminishes as a consequence of $\sin^2 \theta_{13} \neq 0$, while the maximal allowed value is unaltered.

For $R_{pp} = 0.68$, the inclusion of $\sin^2 \theta_{13} \neq 0$ in the analysis leads to a reduction of both the minimal and maximal allowed values of $\sin^2 \theta_{12}$.

For $R_{pp} = 0.72$ and 0.68 cases we also note that the minimal value of $\sin^2 \theta_{12}$ increases as the error in R_{pp} increases and the SNO data begins to have a greater influence on the fit. Thus, the effect of the uncertainty due to $\sin^2 \theta_{13}$ on the precision of $\sin^2 \theta_{12}$ measurement decreases as the error in the pp rate increases.

Figure 8 shows the corresponding sensitivity plot of $\sin^2 \theta_{12}$ from a 3-neutrino oscillation analysis of the global neutrino oscillation data including both the (hypothetical) pp rate data and the prospective data (and errors) from phase-III of the SNO experiment. The corresponding allowed ranges and spread of $\sin^2 \theta_{12}$ is given in columns 5 and 6 of Table 3.

From the expression of the 3-neutrino oscillation probability, eq. (13), we see that the factor $\cos^4 \theta_{13}$ acts like a 'normalization constant'. Since the current 3 limit on this parameter is $\sin^2 \theta_{13} < 0.05$, one would get a 10% uncertainty in P_{ee}^3 and would expect similar uncertainty to appear in the value of $\sin^2 \theta_{12}$ determined using the pp rate. The actual increase in the $\sin^2 \theta_{12}$ uncertainty due to $\sin^2 \theta_{13} \neq 0$ is smaller than 10%, typically being 3% for the plausible values of the pp rate ($R_{pp} = 0.72$) we have considered. Even for the limiting case of $R_{pp} = 0.68$, the maximal increase is by 6%.

The main reason for this is that when we include both "low" and "high" energy experiments in the global analysis there are two conflicting trends. While a non-zero value of $\sin^2 \theta_{13}$ would have a tendency to lower the value of $\sin^2 \theta_{12}$ determined from a 2-neutrino oscillation analysis of the data from the pp experiment, but it would also have a tendency to increase the value of $\sin^2 \theta_{12}$ determined from the data of SNO and SK (i.e., ${}^8\text{B}$ neutrino) experiments. At the lower bound, in general, pp tries to shift the fit to non-zero $\sin^2 \theta_{13}$ and hence lower values of $\sin^2 \theta_{12}$ but the global data including SNO prevents that. On the other hand, at the upper bound, in general, SNO can push the fit to $\sin^2 \theta_{13} \neq 0$ and higher $\sin^2 \theta_{12}$ but pp prefers to keep it at $\sin^2 \theta_{13} = 0.0$ which corresponds to a lower maximal allowed value of $\sin^2 \theta_{12}$.

The uncertainty in the value of $\sin^2 \theta_{13}$ leads to an error in $\sin^2 \theta_{12}$ at the few percent level only when $\sin^2 \theta_{12}$ is determined using data on the pp rate together with the global solar and reactor neutrino data. Nevertheless, the spread in the value of $\sin^2 \theta_{12}$ remains well above 12.5% and

typically exceeds 16% at 3 . As we will show in the next section, $\sin^2 \theta_{12}$ could be measured with a considerably higher precision in a reactor neutrino experiment with a baseline tuned to SPM IN .

pp rate	% error	solar+ reactor + pp		solar(SNO 3)+ reactor+ pp	
		3 range	spread	3 range	spread
0.68	1	0.24 - 0.37	21.3%	0.24 - 0.35	18.6%
	2	0.23 - 0.37	23.3%	0.24 - 0.35	18.6%
	3	0.23 - 0.37	23.3%	0.23 - 0.35	20.7%
	4	0.23 - 0.37	23.3%	0.23 - 0.35	20.7%
0.72	1	0.225 - 0.32	17.4%	0.23 - 0.32	16.4%
	2	0.22 - 0.34	21.4%	0.23 - 0.33	17.9%
	3	0.22 - 0.34	21.4%	0.22 - 0.33	20.0%
	4	0.22 - 0.35	22.8%	0.22 - 0.34	21.4%
0.77	1	0.2 - 0.27	14.9%	0.20 - 0.27	14.9%
	2	0.21 - 0.30	17.6%	0.21 - 0.29	16.0%
	3	0.21 - 0.32	20.8%	0.21 - 0.31	19.2%
	4	0.21 - 0.33	22.2%	0.21 - 0.32	20.8%

Table 3: The 3 allowed ranges and % spread of $\sin^2 \theta_{12}$, obtained from a 3-neutrino oscillation analysis of the global solar and reactor neutrino data, including the hypothetical data on the pp rate.

4 Measuring θ_{12} in a Reactor Experiment at SPM IN

In this section we investigate the possibility of measuring the solar neutrino mixing parameter $\sin^2 \theta_{12}$ in a reactor e^- oscillation experiment, in which the baseline is chosen to correspond to a minimum of the e^- survival probability (SPM IN) [14]. We will consider in what follows an experiment similar to KamLAND , but with a baseline tuned to the SPM IN . The condition of SPM IN reads

$$L_{\text{min}} = 1.24 \frac{E = M \text{ eV}}{m_{21}^2 = \text{eV}^2} \quad (17)$$

For the "old" low-LMA best-fit value of $m_{21}^2 = 7.2 \cdot 10^{-5} \text{ eV}^2$, the baseline which allows the most accurate measurement of $\sin^2 \theta_{12}$ was found to be 70 km [14]. For these m_{21}^2 and baseline the SPM IN appears at the prompt e^+ energy of $E_{\text{vis}} = 3.2 \text{ M eV}$ ⁸, $E_{\text{vis}} = E = 0.8 \text{ M eV}$. The latter corresponds to the maximum of the e^+ (event) spectrum in the absence of oscillations. Obviously, the energy $E_{\text{vis}} = 3.2 \text{ M eV}$, is the most relevant for the statistics of the experiment. We will show in this section that for the current global best-fit value of $m_{21}^2 = 8.3 \cdot 10^{-5} \text{ eV}^2$, $\sin^2 \theta_{12}$

⁸For the details of our reactor code and statistical analysis see refs. [14, 40, 17].

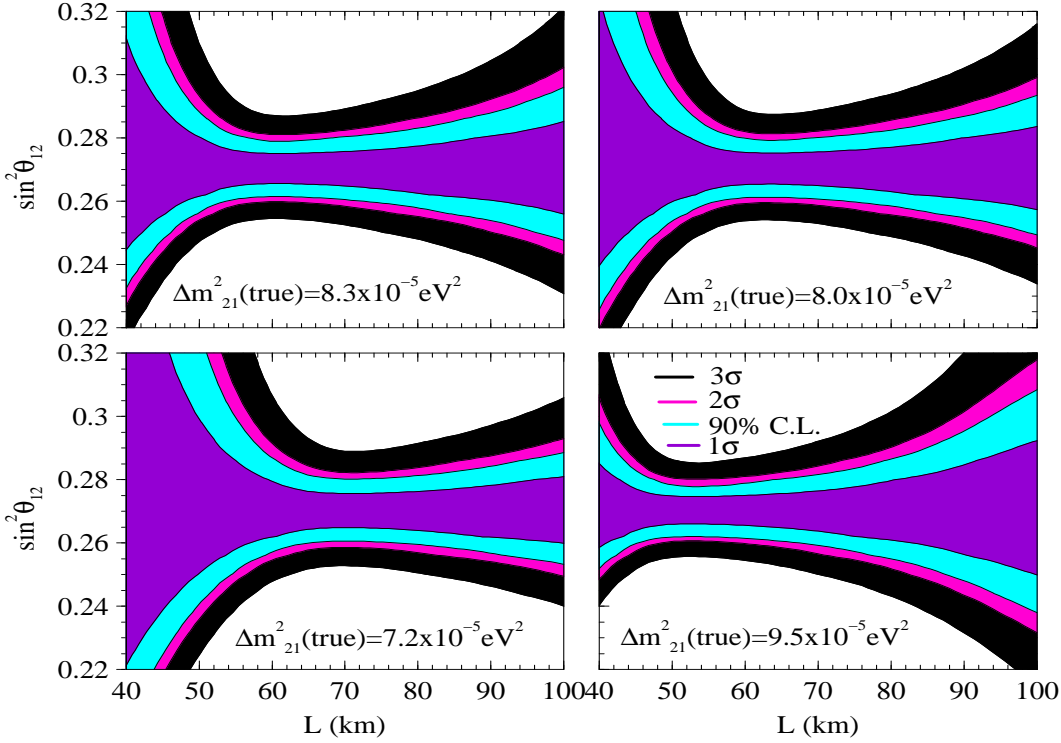


Figure 9: Sensitivity plots showing the 1σ , 2σ , and 3σ range of allowed values for $\sin^2 \theta_{12}$ as a function of the baseline L . The 4 panels are for 4 different true values of Δm^2_{21} . The true value of $\sin^2 \theta_{12}$ is assumed to be 0.27 in all the cases. The Δm^2_{21} is allowed to vary freely in the fit.

could be measured with an accuracy of 2% (6%) at 1 (3) if the baseline chosen is $L = 60$ km. For $\Delta m^2_{21} = 8.3 \times 10^{-5} \text{ eV}^2$ and $L = 60$ km, the SPM IN appears at $E_{\text{vis}} = 3.2 \text{ MeV}$ in the e^+ spectrum. We extend our earlier work [14, 40, 17] by investigating in detail the dependence of the precision of $\sin^2 \theta_{12}$ measurement on the true value of Δm^2_{21} , the baseline, the statistics and on the systematic error of the experiment. We obtain results assuming 2-neutrino oscillations and compare them with the results of a 3-neutrino oscillation analysis. In the latter $\sin^2 \theta_{13}$ is allowed to vary freely within its currently allowed range. We discuss also the relevance of the geo-neutrino flux for the precision of $\sin^2 \theta_{12}$ measurement.

4.1 Sensitivity to $\sin^2 \theta_{12}$ and the Baseline of the Experiment

In Fig. 9 we show the sensitivity to $\sin^2 \theta_{12}$, expected in a reactor experiment, as a function of the baseline L . We assume a total systematic uncertainty of 2% and consider statistics of 73 GW kTy (given as a product of reactor power in GW and the exposure of the detector in kTy). The detector material composition is assumed to be the same as that of KamLAND and so the detector considered has the same number of target protons per kton as KamLAND. The total reactor power, the detector size and the exposure time are kept the same for all baselines. Thus, for longer baseline the number of events would decrease as L^{-2} . We assume that the true value

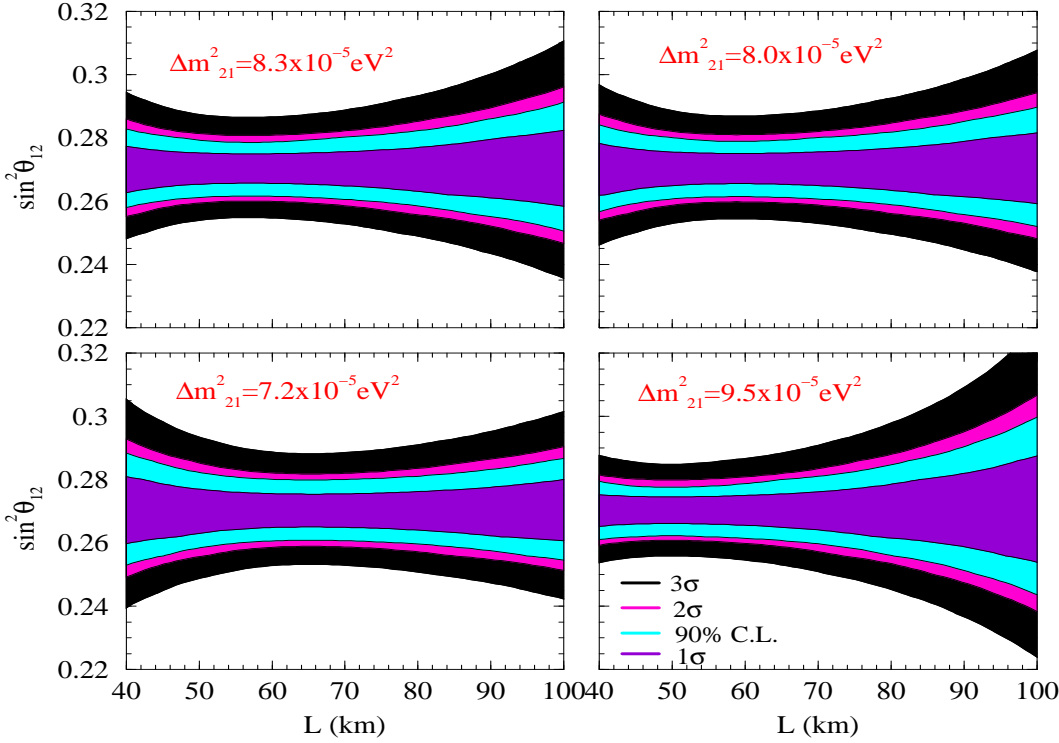


Figure 10: The same as in Fig. 9, but for fixed m_{21}^2 having an assumed true value indicated in each of the panels of the figure.

of $\sin^2 \theta_{12} = 0.27$ and simulate the prospective observed positron spectrum in the detector for four different assumed true values of m_{21}^2 . This figure is obtained for $\sin^2 \theta_{13} = 0$.

We define a χ^2 function given by

$$\chi^2 = \sum_{i,j}^X (N_i^{\text{data}} - N_i^{\text{theory}})^2 / \sigma_{ij}^2 = \sum_{i,j}^X (N_i^{\text{data}} - N_i^{\text{theory}})^2 / (N_{ij}^{\text{data}} - N_{ij}^{\text{theory}})^2; \quad (18)$$

where N_i ($= \text{data}; \text{theory}$) is the number of events in the i^{th} bin, σ_{ij}^2 is the covariant error matrix containing the statistical and systematic errors and the sum is over all bins. We use this χ^2 to fit the simulated spectrum data and get the "measured" value of $\sin^2 \theta_{12}$, keeping m_{21}^2 free. We simulate the spectrum at each baseline and plot the range of values of $\sin^2 \theta_{12}$ allowed by the simulated data as a function of the baseline. The baseline at which the band of allowed values of $\sin^2 \theta_{12}$ is most narrow is the "ideal" baseline for the SPM IN reactor experiment. The figure confirms that this "ideal" baseline depends critically on the true value of m_{21}^2 (cf. eq. (17)). The optimal baseline for the true value of $m_{21}^2 = 8.3 \times 10^{-5} \text{ eV}^2$ is seen from Fig. 9 to be 60 (63) km, while for the "old" low-LMA best-fit value of $m_{21}^2 = 7.2 \times 10^{-5} \text{ eV}^2$ the best baseline would be 70 km. At the optimal baseline the SPM IN reactor experiment can achieve an unprecedented accuracy of 2% (6%) at 1 (3) in the measurement of $\sin^2 \theta_{12}$.

Figure 9 suggests that the optimal baseline for a given true value of m_{21}^2 is very finely tuned. For instance, if for m_{21}^2 (true) = $8.3 \times 10^{-5} \text{ eV}^2$ we change the baseline from $L = 60$ to $L = 50$

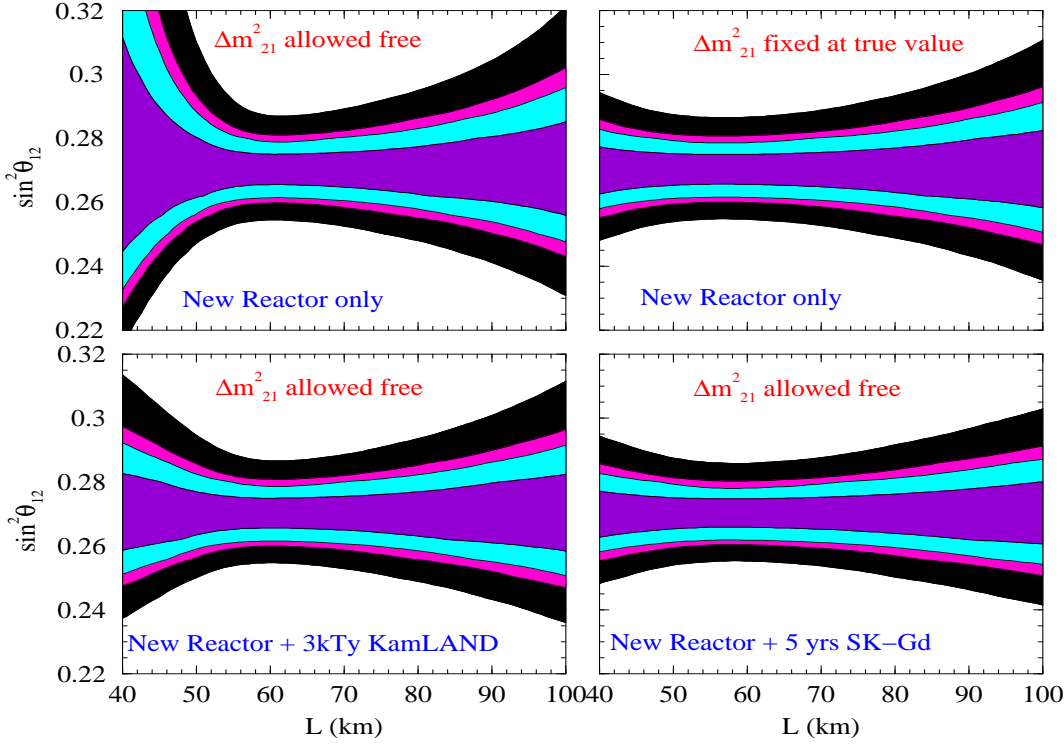


Figure 11: Sensitivity plots showing the 1, 1:64, 2, and 3 range of allowed values for $\sin^2 \theta_{12}$ as a function of the baseline L . The true values of m_{21}^2 (true) = $8.3 \times 10^{-5} \text{ eV}^2$ and of $\sin^2 \theta_{12}$ (true) = 0.27 for all panels. The upper left hand (right hand) panel is obtained allowing m_{21}^2 to vary freely (for fixed m_{21}^2 (true) = $8.3 \times 10^{-5} \text{ eV}^2$). The results shown in the lower left hand (lower right hand) panel are from combined analysis of 3 kTy data from KamLAND (5 year data from the proposed SK-Gd experiment) and 73 GW kTy data from a SPM IN reactor experiment.

km, the sensitivity in $\sin^2 \theta_{12}$ decreases from 2% (6%) to 3% (11%) at 1 (3). However, note that Fig. 9 was obtained by allowing m_{21}^2 to vary freely. This is equivalent to assuming that both $\sin^2 \theta_{12}$ and m_{21}^2 are determined in the reactor SPM IN experiment. For some baselines, especially at smaller L , the oscillation induced spectral distortion is not large enough to measure m_{21}^2 sufficiently accurately, while for the longer baselines the statistics is lower. These factors lead to a certain uncertainty in the determination of m_{21}^2 with the experimental set-up under discussion. The uncertainty in the m_{21}^2 determination translates into additional uncertainty in the measured $\sin^2 \theta_{12}$. If m_{21}^2 could be measured with a sufficiently high precision in an independent experiment, the uncertainty in $\sin^2 \theta_{12}$ due to m_{21}^2 would be reduced.

Figure 10 represents a sensitivity plot similar to that shown in Fig. 9, but obtained for m_{21}^2 fixed at its assumed true value (indicated on each of the panels). As Fig. 10 shows, for fixed m_{21}^2 assumed to have been determined with a sufficiently high precision in an independent experiment, the choice of the baseline for setting up the SPM IN experiment becomes broader. It follows from Fig. 10 that for m_{21}^2 (true) = $8.3 \times 10^{-5} \text{ eV}^2$, for instance, the change of the baseline from $L = 60$ to $L = 70$ km, leads to a minor increase of the uncertainty in the value of $\sin^2 \theta_{12}$ from 6.1% to

6.3% at 3 σ .

It is actually quite possible that m_{21}^2 will be measured with a rather high accuracy in the future. The KamLAND experiment could determine m_{21}^2 with an error of about 7% (at 3 σ) using data of 3 kT_y [26, 14, 12]. The proposed SK-Gd experiment [41] has the potential of measuring the value of m_{21}^2 with an error of 2–3% (at 3 σ) [17]. In Fig. 11 we show the sensitivity to $\sin^2 \theta_{12}$ expected if we combine the SPM IN reactor data with 3 kT_y prospective data from KamLAND (lower left panel) and simulated 5 year data from the proposed SK-Gd experiment (lower right panel). The upper panels were obtained using data from the SPM IN reactor experiment alone. For all the panels we have assumed m_{21}^2 (true) = 8.3×10^{-5} eV². In the upper left panel we allow m_{21}^2 to vary freely, while in the upper right panel m_{21}^2 is fixed at the assumed true value. We note that if the SPM IN reactor data is combined with 5 year data from the SK-Gd experiment, the choice of optimal baseline is much wider since m_{21}^2 would be determined with a relatively high precision by the SK-Gd experiment. With the addition of the SK-Gd results to the total data set, the spread in $\sin^2 \theta_{12}$ is 5.7% at 3 σ . The combined SPM IN reactor and KamLAND 3 kT_y data would yield an uncertainty in the value of $\sin^2 \theta_{12}$ of 5.9% at 3 σ . Since the analysis of the combined KamLAND (or SK-Gd) and SPM IN reactor data confirms that the effect of m_{21}^2 on the $\sin^2 \theta_{12}$ sensitivity can be negligible, we will take m_{21}^2 to be fixed for the remainder of this section.

4.2 Impact of Statistical and Systematic Errors on $\sin^2 \theta_{12}$ Sensitivity

One of the important requirements for the type of high precision experiment we are discussing is the accumulation of relatively high statistics in a reasonable period of time. Since the statistics falls as L^{-2} and since rather long baselines are required for a precision measurement of the solar neutrino oscillation parameters, for a given reactor power longer baselines would imply bigger detectors and larger exposure times. Thus, the question about the dependence of the precision of measurement of $\sin^2 \theta_{12}$ in a reactor SPM IN experiment on the statistics of the experiment naturally arises. In Fig. 12 we show the effect of the statistics on the $\sin^2 \theta_{12}$ sensitivity in the case of m_{21}^2 (true) = 8.3×10^{-5} eV². The four panels are obtained for four different sample baselines of 50, 60, 70 and 80 km. The range of allowed values of $\sin^2 \theta_{12}$ is shown as a function of the product of reactor power and the detector mass and exposure time. For $L = 60$ km, for instance, the uncertainty in $\sin^2 \theta_{12}$ diminishes from 3% (10%) to 2% (6%) at 1 (3) σ as the statistics is increased from 20 GW kT_y to 60 GW kT_y. Note that the difference in the $\sin^2 \theta_{12}$ precision for 60 GW kT_y and 73 GW kT_y (used in Figs. 9 and 10) is marginal, and shows up only in the first place in decimal in the value of the spread.

Another important aspect which determines the potential of the experiment for precision measurement of $\sin^2 \theta_{12}$ is the systematic uncertainty. Obviously, smaller systematic errors are preferable. All the plots presented so far in this section have been generated with an assumed 2% systematic error. The systematic uncertainty in the KamLAND experiment is about 6.5%. Most of it comes from the uncertainty in the detector fiducial mass and the reactor power. Our choice of 2% for the systematic error is based on the optimistic assumption that the error in the flux normalization could be reduced sufficiently by using the near-far detector set-up. One could envisage the θ_{12} reactor SPM IN experiment as a second leg of a reactor experiment dedicated to measure

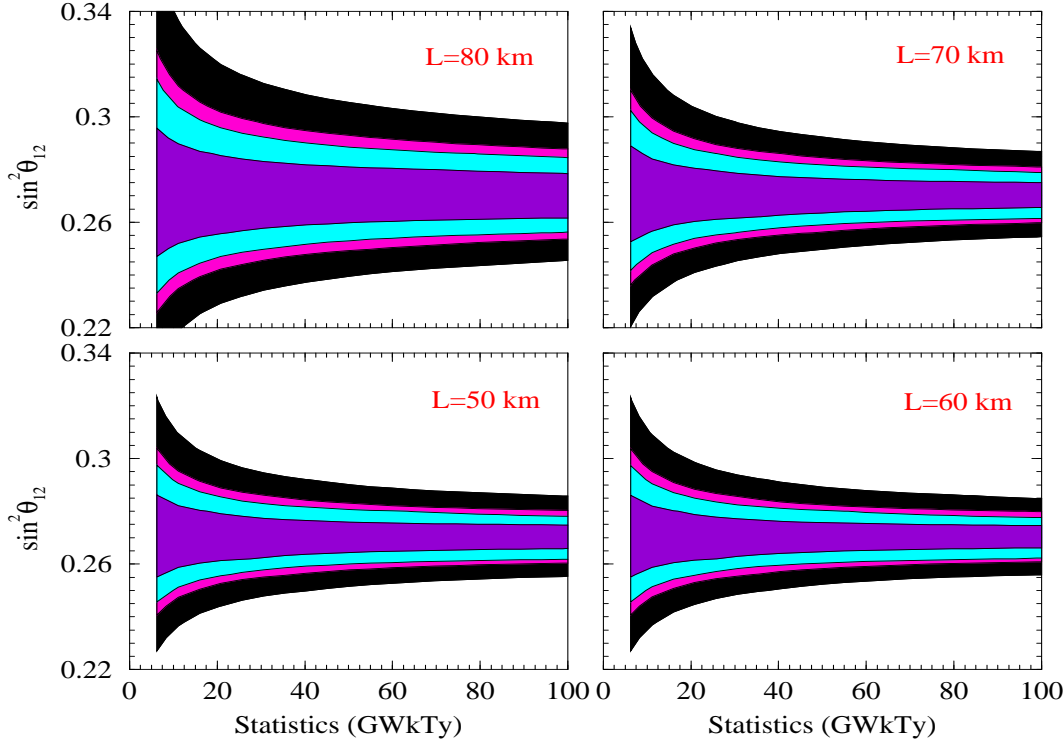


Figure 12: Sensitivity plots showing the 1σ , $1:64\sigma$, 2σ , and 3σ ranges of allowed values for $\sin^2 \theta_{12}$ as a function of the statistics in units of GW kTy. All the four panels correspond to a fixed value of $m_{21}^2 = 8.3 \times 10^{-5} \text{ eV}^2$.

θ_{13} (see, e.g., [42]). The detector for measuring θ_{13} could then effectively be used as near detector for the long baseline SPM IN experiment for high precision measurement of θ_{12} . It should be added that the errors due to the uncertainties in the threshold energy and ν_e spectrum have also to be reduced to achieve the systematic error of 2%. Experimentally this could be a very challenging task.

Since systematic uncertainties may be difficult to reduce in the experiment under discussion, we estimate next how much the precision on $\sin^2 \theta_{12}$ deteriorates as the systematic error increases. Figure 13 shows the effect of increasing the systematic error from the 2% assumed by us to the rather conservative value of 5%. For $m_{21}^2(\text{true}) = 8.3 \times 10^{-5} \text{ eV}^2$, the spread in $\sin^2 \theta_{12}$ at $L = 60 \text{ km}$ increases from 6.1% to 8.6% at 3σ , as the systematic error is increased from 2% to 5%. We conclude that the effect of systematic uncertainty on the precision of $\sin^2 \theta_{12}$ measurement is important, but its impact is not dramatic as long as the systematic error does not exceed 5%. Similar conclusion regarding the effect of a 4% systematic error on the accuracy of $\sin^2 \theta_{12}$ determination in the SADO experiment was reached in [16].

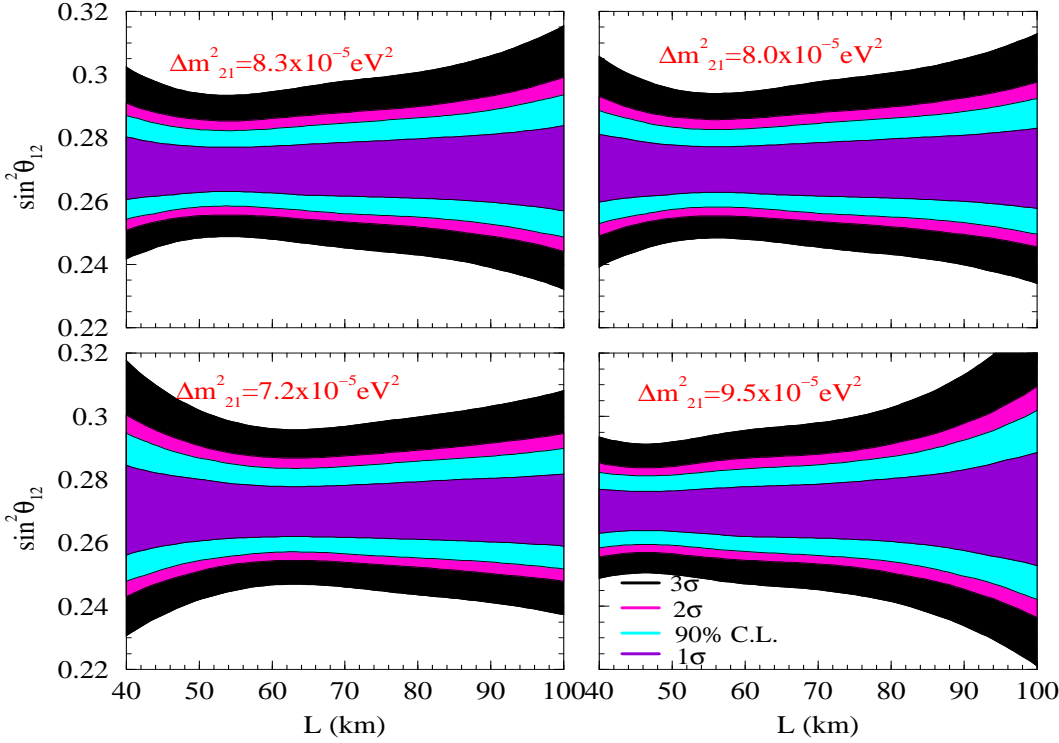


Figure 13: The same as in Fig. 10 but for a systematic uncertainty of 5% .

4.3 The Uncertainty Due to $\sin^2 \theta_{13}$

As we have discussed earlier in connection with the KamLAND experiment, the 3-neutrino oscillation survival probability for the reactor e of interest is given by

$$P_{ee} = \cos^4 \theta_{13} (1 - \sin^2 2 \theta_{12} \sin^2 \frac{m_{21}^2 L}{4E})^{\frac{1}{2}}; \quad (19)$$

where the term $\sin^4 \theta_{13}$ has been neglected. Therefore the uncertainty in $\sin^2 \theta_{13}$, eq. (12), brings up to a 10% uncertainty in the value of the e survival probability. Since the factor $\cos^4 \theta_{13}$ can only reduce the survival probability, it does not affect the upper limit of the allowed range of $\sin^2 \theta_{12}$. However, it can have an effect on the minimal allowed value of $\sin^2 \theta_{12}$ reducing it further, and thus can worsen, in principle, the precision of the experiment to $\sin^2 \theta_{12}$.

The additional error on $\sin^2 2 \theta_{12}$ coming from the uncertainty in $\sin^2 \theta_{13}$ can be roughly estimated using eq. (19) as [40],

$$(\sin^2 2 \theta_{12}) = \frac{2 P_{ee} \sin^2 \theta_{13}}{\sin^2 \frac{m_{21}^2 L}{4E}} + 2 \frac{(1 - \sin^2 2 \theta_{12} \sin^2 \frac{m_{21}^2 L}{4E}) (\sin^2 \theta_{13})}{\sin^2 \frac{m_{21}^2 L}{4E}}; \quad (20)$$

where P_{ee} and $(\sin^2 \theta_{13})$ are the uncertainties in the determination of the survival probability and $\sin^2 \theta_{13}$, respectively. In the SPM IN region we are interested in one has $\sin^2 (m_{21}^2 L/4E) \approx 1$

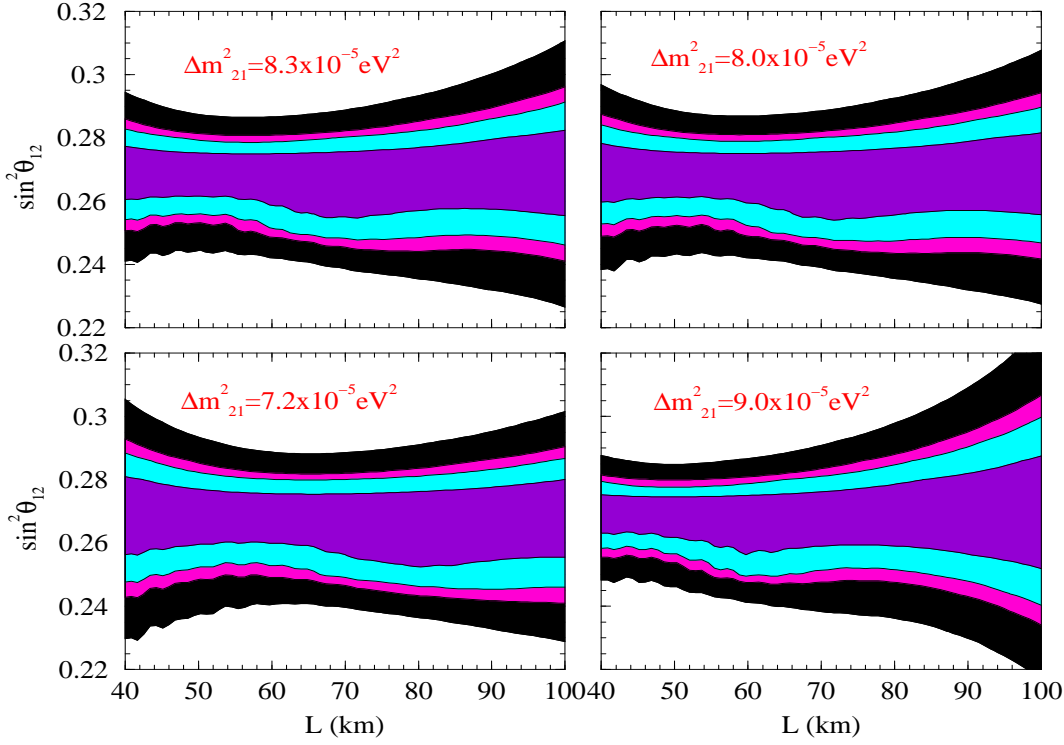


Figure 14: The same as in Fig. 10 but for a 3-neutrino oscillation analysis in which $\sin^2 \theta_{13}$ is allowed to vary freely within its current 3 allowed range.

and therefore

$$(\sin^2 2 \theta_{12}) = 2 P_{ee} \sin^2 \theta_{13} + 2 \cos^2 2 \theta_{12} (\sin^2 \theta_{13}) : \quad (21)$$

Thus, for a reactor SPM IN set-up, the first term gives an extra contribution of about $2 P_{ee} \sin^2 \theta_{13}$ to the allowed range of $\sin^2 2 \theta_{12}$. Even under the most conservative conditions one can expect that $P_{ee} < 0.1$, so this term could give an additional contribution of < 0.01 to the allowed range of $\sin^2 2 \theta_{12}$. The second term is independent of the precision of a given experiment. It depends only on the best-fit value of $\cos^2 2 \theta_{12}$ and on the uncertainty in $\sin^2 \theta_{13}$. For the current 3 upper limit on $\sin^2 \theta_{13}$ of 0.05 and best-fit value of $\cos^2 2 \theta_{12} = 0.19$, the second term would lead to an increase in the uncertainty in $\sin^2 2 \theta_{12}$ by about 0.02 only. The suppression of this term is mainly due to the presence of the $\cos^2 2 \theta_{12}$ factor, which is relatively small for the current best-fit value. Thus, even though the current uncertainty in $\sin^2 \theta_{13}$ brings a 10% uncertainty in the value of P_{ee} , it increases the allowed range of $\sin^2 2 \theta_{12}$ only by a few %, if one uses a reactor experiment with a baseline tuned to the SPM IN for a high precision measurement of $\sin^2 2 \theta_{12}$.

The above conclusions are illustrated in Fig. 14 showing the uncertainty in $\sin^2 \theta_{12}$ expected in the case when θ_{13} is allowed to vary freely in its currently allowed range of $\sin^2 \theta_{13} < 0.05$. The figure shows that the upper bound on $\sin^2 \theta_{12}$ remains unaffected by the $\sin^2 \theta_{13}$ uncertainty, while the minimal allowed value diminishes somewhat, increasing the uncertainty in $\sin^2 \theta_{12}$. However, for the baseline which corresponds to the SPM IN, the sensitivity reduces only by 2–3% in spite

of the 10% uncertainty in $\sin^2 \theta_{13}$. For m_{21}^2 (true) = 8.3×10^{-5} eV², for instance, the uncertainty in $\sin^2 \theta_{12}$ increases from 6.1% to 8.7% at 3%.

4.4 On the Impact of Geo-Neutrino Flux

Our Earth is known to be a huge heat reservoir and is estimated to radiate about 40 TW of heat. A large fraction (16%) of this is believed to be radiogenic in origin, coming from the decay chain of ²³⁸U, ²³²Th and ⁴⁰K. The radioactive decays of these isotopes produce antineutrinos in the beta decay processes of their decay chains. These $\bar{\nu}_e$ coming from inside the Earth are usually called Geo-neutrinos ($\bar{\nu}_e^{\text{geo}}$) [43]. The maximum energy of the $\bar{\nu}_e^{\text{geo}}$ produced in the ⁴⁰K decay chain is only $E_{\bar{\nu}_e} = 1.31$ MeV, which is below the detection energy threshold of $\bar{\nu}_e$ in scintillation detectors of the type of KamLAND we are considering. However, the $\bar{\nu}_e^{\text{geo}}$ from ²³⁸U and ²³²Th have maximum energy of $E_{\bar{\nu}_e} = 3.26$ MeV and $E_{\bar{\nu}_e} = 2.25$ MeV, respectively, and can be observed in scintillation detectors.

The flux of $\bar{\nu}_e^{\text{geo}}$ is unknown. Even the total heat radiated by Earth has a rather large uncertainty: it could be 31–40 TW. There is no direct measurement of the abundances of the ²³⁸U and ²³²Th inside the Earth. One can estimate their abundances using the meteoritic and seismic data. This results in the $\bar{\nu}_e^{\text{geo}}$ flux being largely model dependent and uncertain. Most models give the bulk ²³²Th/²³⁸U ratio as ²³²Th/²³⁸U = 3.8. Even the value of this ratio could have a relatively large error (e.g., the authors of [44] estimate this error as 14%). The measurement of the $\bar{\nu}_e^{\text{geo}}$ flux would lead to a better understanding of the interior of the Earth, and is therefore a very important branch of neutrino physics in its own right [45]. As far as the precision measurement of the neutrino oscillation parameters is concerned, the events due to $\bar{\nu}_e^{\text{geo}}$ can be an important background and can lead to an error in the measured value of $\sin^2 \theta_{12}$.

Since the $\bar{\nu}_e^{\text{geo}}$ have a maximum energy of $E_{\bar{\nu}_e} = 3.26$ MeV which corresponds to a prompt e^+ energy of only $E_{\text{vis}} = 2.48$ MeV, one way to avoid the uncertainty due to $\bar{\nu}_e^{\text{geo}}$ is to implement a prompt energy threshold of 2.6 MeV, as is done by the KamLAND collaboration. In this paper we have followed the KamLAND approach. In this case the observed e^+ spectrum does not have any 'contamination' due to contributions from $\bar{\nu}_e^{\text{geo}}$. An alternative approach is to use the entire prompt e^+ energy spectrum in the analysis, taking the $\bar{\nu}_e^{\text{geo}}$ flux into account. Since the theoretical estimates on the $\bar{\nu}_e^{\text{geo}}$ flux are presently rather imprecise, one could let the ²³⁸U and ²³²Th $\bar{\nu}_e^{\text{geo}}$ flux normalisation vary as a free parameter. Both approaches have their merits and drawbacks. In the first approach (we use in this paper), while there are no additional uncertainties due to the unknown $\bar{\nu}_e^{\text{geo}}$ background, one has to contend with the experimental challenge of understanding and reducing the error associated with the prompt e^+ threshold energy.⁹ In the second approach there is no prompt e^+ energy cut, but one has to handle the uncertainty due to the lack of knowledge of $\bar{\nu}_e^{\text{geo}}$ background. Keeping the ²³⁸U and ²³²Th $\bar{\nu}_e^{\text{geo}}$ flux normalisation as free parameter brings in extra error in the measurement on $\sin^2 \theta_{12}$.

The key feature in the ₁₂ SPM IN reactor experiment proposed in [44], is the appearance of SPM IN in the observed e^+ spectrum. If the SPM IN appears at a prompt energy of $E_{\text{vis}} > 2.6$

⁹In the case of KamLAND experiment the uncertainty in the e^+ threshold energy corresponds to a systematic error 2%.

M eV, implementing a threshold of $E_{\text{vis}} = 2.6$ M eV ¹⁰ and thus avoiding the e^{geo} background might permit to measure $\sin^2 \theta_{12}$ with the highest precision, achievable in the experiment under discussion. If, on the other hand, SPM IN appears at $E_{\text{vis}} < 2.6$ M eV, the entire e^+ energy spectrum would have to be taken into account and in this case the e^{geo} background cannot be avoided. For a given value of m^2_{21} , the position of the SPM IN in the e^+ spectrum depends on the baseline of the experiment. For shorter baselines, SPM IN occurs at smaller energies. Therefore the choice of the baseline of the experiment would determine whether one would have to take the e^{geo} background into account or not.

The authors of [16] have included the e^{geo} background in their analysis of the $\sin^2 \theta_{12}$ precision expected in the SADO experiment in Japan with a baseline of $L = 54$ km. They conclude that for this experimental set-up, the e^{geo} background does not have significant impact on the precision of $\sin^2 \theta_{12}$ measurement. For $L = 54$ km, the SPM IN is at $E_{\text{vis}} = 2.8$ M eV. The uncertainty in the e^{geo} flux does not make much impact in this case since $E_{\text{vis}} = 2.8$ M eV is larger than the background e^{geo} energies. For shorter baselines the SPM IN will take place at $E_{\text{vis}} < 2.6$ M eV and the uncertainty due to the e^{geo} flux can affect noticeably the precision of measurement of $\sin^2 \theta_{12}$.

5 Conclusions

We have investigated the possibilities of high precision measurement of the solar neutrino mixing angle θ_{12} in solar and reactor neutrino experiments. As a first step, we have analyzed the improvements in the determination of $\sin^2 \theta_{12}$, which can be achieved with the expected increase of statistics and reduction of systematic errors in the currently operating solar and KamLAND experiments. With the phase-III prospective data from SNO experiment included in the current global solar neutrino and KamLAND data, the uncertainty in the value of $\sin^2 \theta_{12}$ is expected to diminish from 24% to 21% at 3 σ . If instead of 766.3 kT γ , one uses simulated 3 kT γ KamLAND data in the same analysis, the 3 σ error in $\sin^2 \theta_{12}$ reduces to 18%.

We next considered the potential of a generic LowNu e elastic scattering experiment, designed to measure the pp solar neutrino flux, for high precision determination of $\sin^2 \theta_{12}$. We examined the effect of including values of the pp neutrino induced electron scattering rates in the χ^2 analysis of the global solar neutrino data. Three representative values of the rates from the currently allowed 3 σ range were considered: 0.68, 0.72, 0.77. The error in the measured rate was varied from 1% to 5%. By adding the pp flux data in the analysis, the error in $\sin^2 \theta_{12}$ determination reduces to 14% (19%) at 3 σ for 1% (3%) uncertainty in the measured pp rate. Performing a similar three-neutrino oscillation analysis we found that, as a consequence of the uncertainty on $\sin^2 \theta_{13}$, the error on the value of $\sin^2 \theta_{12}$ increases correspondingly to 17% (21%).

We also studied the possibility of a high precision determination of $\sin^2 \theta_{12}$ in a reactor experiment with a baseline corresponding to a Survival Probability Measurement (SPM IN). We showed that in a $L = 60$ km experiment with statistics of 60 G W kT γ and systematic error of 2%, $\sin^2 \theta_{12}$ could be measured with an uncertainty of 2% (6%) at 1 σ (3 σ). The inclusion of the $\sin^2 \theta_{13}$ uncer-

¹⁰This will increase the systematic uncertainty due to the error from the prompt e^+ energy cut. We have shown that the impact of the increase of the systematic uncertainty on the precision of $\sin^2 \theta_{12}$ determination is relatively small as long as the systematic error does not exceed 5%.

tainty in the analysis changes this error to 3% (9%). An independent determination of m_{21}^2 with sufficiently high accuracy would allow, as we have shown, \sin^2_{12} to be measured with the highest precision over a relatively wide range of baselines. We investigated in detail the dependence of the precision on \sin^2_{12} which can be achieved in such an experiment on the baseline, statistics and systematic error. More specifically, with the increase of the statistics from 20 GW kT γ to 60 GW kT γ , the error diminishes from 3% (10%) to 2% (6%) at 1 (3). For statistics of (60 – 70) GW kT γ , the increase of the systematic error from 2% to 5% leads to an increase in the uncertainty in \sin^2_{12} from 6% to 9% at 3.

We have found that the effect of \sin^2_{13} uncertainty on the \sin^2_{12} determination in LowNuPP and SPM IN reactor experiments considered is considerably smaller than naively expected.

The results of our analyses for the currently running, the proposed LowNu and future reactor experiments show that the most precise determination of \sin^2_{12} can be achieved in a dedicated reactor experiment with a baseline tuned to SPM IN associated with $m_{21}^2 \approx m^2$.

Acknowledgments: We would like to thank Y. Suzuki, A. Suzuki, M. Nakahata, F. Suekane, and C. Pena-Garay for useful discussions. This work was supported by the Italian INFN under the program "Fisica Astroparticellare" (S.C. and S.T.P.).

References

- [1] B.T. Cleveland et al., *Astrophys. J.* **496**, 505 (1998).
- [2] J.N. Abdurashitov et al. [SAGE Collaboration], *J. Exp. Theor. Phys.* **95**, 181 (2002) [Zh. Eksp. Teor. Fiz. **122**, 211 (2002)] [[arXiv:astro-ph/0204245](https://arxiv.org/abs/astro-ph/0204245)].; W. Hampel et al. [GALLEX Collaboration], *Phys. Lett. B* **447**, 127 (1999); C. Cattadori, Talk at Neutrino 2004, Paris, France, June 14–19, 2004 (<http://neutrino2004.in2p3.fr>).
- [3] S. Fukuda et al. [Super-Kamiokande Collaboration], *Phys. Lett. B* **539**, 179 (2002).
- [4] Q.R. Ahmad et al. [SNO Collaboration], *Phys. Rev. Lett.* **89**, 011301 (2002). Q.R. Ahmad et al. [SNO Collaboration], *Phys. Rev. Lett.* **89**, 011302 (2002) [[arXiv:nucl-ex/0204009](https://arxiv.org/abs/nucl-ex/0204009)].
- [5] S.N. Ahmed et al. [SNO Collaboration], *Phys. Rev. Lett.* **92**, 181301 (2004).
- [6] E. Kearns, talk at Neutrino 2004, Paris, (<http://neutrino2004.in2p3.fr>).
- [7] K. Eguchi et al., [KamLAND Collaboration], *Phys. Rev. Lett.* **90** (2003) 021802.
- [8] M.H. Ahn et al., *Phys. Rev. Lett.* **90** (2003) 041801.
- [9] T. Araki et al., [KamLAND Collaboration], [hep-ex/0406035](https://arxiv.org/abs/hep-ex/0406035).
- [10] T.Nakaya et al., talk given at '04 International Conference, June 14–19, 2004, Paris, France (<http://neutrino2004.in2p3.fr>).
- [11] V. Gribov and B. Pontecorvo, *Phys. Lett. B* **28**, 493 (1969).

[12] A .Bandyopadhyay, S .Choubey, S .G oswam i, S .T .Petcov and D .P .Roy, [hep-ph/0406328](#).

[13] M .M altoni, T .Schwetz, M .A .Tortola and J.W .F .Valle, [arX iv:hep-ph/0405172](#); J.N .Bahcall, M .C .G onzalez-G arcia and C .Pena-G aray, *JHEP* 0408, 016 (2004); P .A liani, V .A ntonelli, R .F errari, M .P icariello and E .Torrente-Lujan, [arX iv:hep-ph/0406182](#).

[14] A .Bandyopadhyay, S .Choubey and S .G oswam i, *Phys. Rev. D* 67, 113011 (2003).

[15] A .Bandyopadhyay, S .Choubey, S .G oswam i and S .T .Petcov, *Phys. Lett. B* 581, 62 (2004).

[16] H .M inakata, H .N unokawa, W .J .C .Teves and R .Zukanovich Fundhal, [arX iv:hep-ph/0407326](#).

[17] S .Choubey and S .T .Petcov, *Phys. Lett. B* 594, 333 (2004).

[18] R .S .Raghavan, Talk given at the Int. W orkshop on Neutrino Oscillations and their Origin (NOON 2004), February 11 – 15, 2004, Tokyo, Japan; for further information see the web-site: <http://www.phys.vt.edu/~kimballton/> .

[19] M .N akahata, Talk given at the Int. W orkshop on Neutrino Oscillations and their Origin (NOON 2004), February 11 – 15, 2004, Tokyo, Japan.

[20] Y .Suzuki, Talk given at '04 International Conference, June 14–19, 2004, Paris, France (<http://neutrino2004.in2p3.fr>).

[21] J .N .Bahcall and C .Pena-G aray, *JHEP* 0311, 004 (2003).

[22] J .N .Bahcall and M .H .P insonneault, *Phys. Rev. Lett.* 92, 121301 (2004).

[23] A .Bandyopadhyay, S .Choubey, S .G oswam i and K .Kar, *Phys. Lett. B* 519, 83 (2001).

[24] A .Bandyopadhyay, S .Choubey, S .G oswam i and D .P .Roy, *Phys. Lett. B* 540, 14 (2002). S .Choubey, A .Bandyopadhyay, S .G oswam i and D .P .Roy, [arX iv:hep-ph/0209222](#).

[25] A .Bandyopadhyay, S .Choubey, S .G oswam i, S .T .Petcov and D .P .Roy, *Phys. Lett. B* 583, 134 (2004).

[26] A .Bandyopadhyay, S .Choubey, R .G andhi, S .G oswam i and D .P .Roy, *J. Phys. G* 29, 2465 (2003) [[arX iv:hep-ph/0211266](#)]. A .Bandyopadhyay, S .Choubey, R .G andhi, S .G oswam i and D .P .Roy, *Phys. Lett. B* 559, 121 (2003).

[27] T .A rakiet al., [hep-ex/0406035](#) (v3).

[28] K evin G raham , talk at NOON 2004, February 11–15, 2004, Tokyo, Japan, <http://www-sk.icrr.u-tokyo.ac.jp/noon2004/>; H . Robertson for the SNO Collaboration, Talk given at TAUP 2003, Univ. of Washington, Seattle, Washington, September 5 – 9, 2003, <http://mocha.phys.washington.edu/taup2003>

[29] M. M. Maris and S.T. Petcov, *Phys. Lett. B* 534, 17 (2002).

[30] S.T. Petcov and J. Rich, *Phys. Lett. B* 224, 401 (1989).

[31] G. L. Fogli and E. Lisi, *Astropart. Phys.* 3, 185 (1995).

[32] S.T. Petcov, *New. J. Phys.* 6 (2004) 109 (<http://stacks.iop.org/1367-2630/6/109>), and Talk given at XX Ist International Conference on Neutrino Physics and Astrophysics (Neutrino-2004), June 14-19, 2004, Paris, France (see <http://neutrino2004.in2p3.fr>).

[33] S. S. Goswami, Global analysis of neutrino oscillation, talk at XX Ist International Conference on Neutrino Physics and Astrophysics (Neutrino-2004), Paris, June 14-19, 2004, see <http://neutrino2004.in2p3.fr>; S. Goswami, A. Bandyopadhyay, S. Choubey [[hep-ph/0409224](http://arXiv:hep-ph/0409224)].

[34] C. Athanassopoulos et al., *Phys. Rev. Lett.* 81 (1998) 1774.

[35] S. Brame et al., Talk given at '04 International Conference, June 14-19, 2004, Paris, France (<http://neutrino2004.in2p3.fr>).

[36] M. Apollonio et al. [CHOOZ Collaboration], *Phys. Lett. B* 466, 415 (1999), and *Eur. Phys. J. C* 27, 331 (2003); F. Boehm et al., *Phys. Rev. D* 64, 112001 (2001).

[37] S.T. Petcov, *Phys. Lett. B* 214, 259 (1988).

[38] S.T. Petcov, *Phys. Lett. B* 200, 373 (1988), and *Phys. Lett. B* 214, 139 (1988); P. I. Krastev and S.T. Petcov, *Phys. Lett. B* 207, 64 (1988); E. Lisi et al., *Phys. Rev. D* 63, 093002 (2000).

[39] A. Bandyopadhyay, S. Choubey, S. Goswami and K. Kar, *Phys. Rev. D* 65, 073031 (2002).

[40] S. Choubey, S.T. Petcov and M. Piai, *Phys. Rev. D* 68, 113006 (2003).

[41] J.F. Beacom and M. R. Vagins, arXiv:hep-ph/0309300.

[42] K. Anderson et al., White Paper Report on Using Nuclear Reactors to Search for ν_{13} , arXiv:hep-ex/0402041.

[43] G. Eder, *Nucl. Phys.* 78, 657 (1966).

[44] G. L. Fogli, E. Lisi, A. Palazzo and A. M. Rotunno, arXiv:hep-ph/0405139.

[45] G. Fiorentini, M. Lissia, F. Mantovani and R. Vannucci, arXiv:hep-ph/0409152. F. Mantovani, L. Caramignani, G. Fiorentini and M. Lissia, *Phys. Rev. D* 69, 013001 (2004); G. Fiorentini, T. Lasserre, M. Lissia, B. Ricci and S. Schonert, *Phys. Lett. B* 558, 15 (2003); H. Nunokawa, W. J. C. Teves and R. Zukanovich Funchal, *JHEP* 0311, 020 (2003).